

Influence of oxygen on the interfacial stability of Cu on Co(0001) thin films

Hongmei Wen,¹ Matthew Neurock,^{1,*} and Haydn N. G. Wadley²

¹Department of Chemical Engineering, University of Virginia, Charlottesville, Virginia 22904-4741, USA

²Department of Materials Science and Engineering, University of Virginia, Charlottesville, Virginia 22904-4741, USA

(Received 16 June 2006; published 2 February 2007)

Vapor deposited Cu/Co multilayers with high quality Co-Cu interfaces exhibit significant giant magnetoresistance. These multilayers are sometimes grown using process environments with significant background partial pressures of oxygen, which can impact the quality of film and its properties. Previously we found that oxygen preferentially stabilizes Co/Cu(111). First principle density functional theoretical calculations are used herein to examine the effects of surface atomic oxygen on the stability of the Cu(111)/Co(0001) interface. This interface can be grown with varying degrees of intermixing at the surface. We examine the significance of this by analyzing the first two Cu layers deposited on a Co(0001) substrate. The effects of oxygen are studied for the nonmixed $\text{Cu}_1 \text{ ML}/\text{Co}_1 \text{ ML}/\text{Co}(0001)$ system, the mixed $\text{Co}_{0.33}\text{Cu}_{0.67}/\text{Co}_{0.67}\text{Cu}_{0.33}/\text{Co}(0001)$ and $\text{Co}_{0.66}\text{Cu}_{0.33}/\text{Co}_{0.33}\text{Cu}_{0.67}/\text{Co}(0001)$ surface alloys and the Co-capped $\text{Co}_1 \text{ ML}/\text{Cu}_1 \text{ ML}/\text{Co}(0001)$ system. In the absence of oxygen, the nonmixed $\text{Cu}_1 \text{ ML}/\text{Co}_1 \text{ ML}/\text{Co}(0001)$ system is found to be the most stable. The calculations show that the fraction of the surface comprised of Cu, in the absence of background oxygen, is maximized for Cu deposited onto a Co(0001) substrate. This reduces the tendency for intermixing. Submonolayer coverages of atomic oxygen preferentially bind at the three-fold fcc and hcp sites on all four Cu/Co(0001) surfaces investigated as well as on the homogeneous Co(0001) and the Cu(111) surfaces. The difference in the oxygen-metal binding energy for the fcc and hcp sites appears to be negligible which is consistent with the minor changes that occur in the local structure (oxygen height above the surface and interlayer spacing). Total energy calculations indicate that the intermixing is unfavorable when the oxygen coverage is kept below 0.362 ML. This threshold coverage is hardly affected by the oxygen binding sites (hcp and fcc), stacking sequence of the metal layer or thicker Cu layers. This threshold oxygen coverage minimizes the influence of the surface oxygen on the magnetic properties of the system. These results, taken with other calculations for Co/Cu(111), suggest that 0.362 ML of oxygen is optimal for stabilizing the Co/Cu(111) interface without disrupting the stability of the Cu/Co(0001) interface. The calculations show that the addition of oxygen to the Cu-segregated unmixed $\text{Cu}_1 \text{ ML}/\text{Co}_1 \text{ ML}/\text{Co}(0001)$ surface increases the surface magnetization as a result of the unpaired electrons that arise from the surface oxygen atoms. The addition of atomic oxygen to the Co-capped $\text{Co}_1 \text{ ML}/\text{Cu}_1 \text{ ML}/\text{Co}(0001)$ surface, on the other hand, results in an increase in the magnetization for oxygen coverages up to 0.33 ML. At higher oxygen coverages, however, there is a shifting of the minority states toward the majority states near the Fermi level which significantly reducing the magnetization of the surface Co layer.

DOI: [10.1103/PhysRevB.75.085403](https://doi.org/10.1103/PhysRevB.75.085403)

PACS number(s): 68.43.-h, 68.55.-a, 68.65.Ac

I. INTRODUCTION

Multilayered cobalt-copper films grown by vapor deposition have attracted a great deal of interest as potential magnetic sensors in ultrahigh-density data storage devices and for future generations of magnetic random access memory.¹ These devices rely on the giant magnetoresistance (GMR) exhibited by these multilayers.^{1,2} The large magnetoresistance is directly related to the spin-dependent scattering of electrons within these magnetic multilayers and is significantly affected by the atomic scale structure and local chemical composition at the interface between the deposited Co and Cu layers. GMR therefore depends on the degree of interfacial roughness as well as the extent of interfacial mixing at the Co on Cu and Cu on Co interfaces in the multilayers.³⁻⁶ Smooth and unmixed Co-Cu interfaces are thought to optimize the magnetoresistance.³ Intermixing is experimentally found to occur predominantly at the Co-on-Cu interface in Co/Cu multilayers.^{3,5,7-13} Recent molecular dynamics simulations and *ab initio* simulations lead to

similar conclusions for other Cu/Co systems.^{14,15} This arises because Cu has a lower surface free energy than Co. Copper is therefore energetically preferred on the growth surface during the deposition of Co on Cu. Recent experimental work has indicated that the addition of small amounts of oxygen during the epitaxial growth of Co and Cu multilayers significantly reduces the degree of interfacial intermixing.^{3,11} The fundamental reasons for this observation are unclear.

Eggelhoff was the first to report that the presence of oxygen within the background gas during deposition improved the magnetoresistance of Co/Cu thin films.¹¹ Subsequent studies have probed this over different Co-Cu thin films in more detail.^{9,12,13,16-21} Several of these studies examined the effects of oxygen on interfacial roughness.^{3,9,11-13,17,18,21} and reported improved surface/interfacial structure, i.e., “flatness,” as a result of more pronounced epitaxial step flow growth and suppression of three-dimensional (3D) island formation. The addition of a half of monolayer of oxygen prior to Co deposition onto Cu was also found to suppress inter-

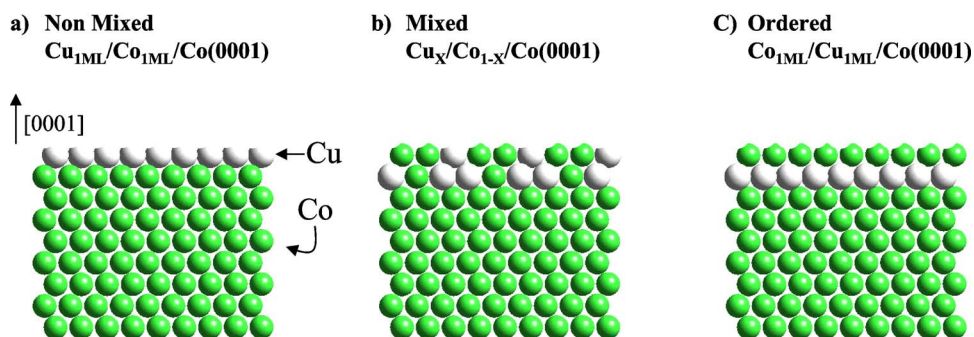


FIG. 1. (Color online) A schematic picture of the Cu-on-Co interfaces: (a) the nonmixed Cu-on-Co interface, (b) the mixed alloy Cu-on-Co interface, and (c) the Co-capped Cu-on-Co interface. Co and Cu are depicted by the green and white spheres, respectively.

mixing of Co in Cu.^{3,9,11,13} In recent (unpublished²²) theoretical work we showed that intermixing at the Co on Cu(111) interface can be reduced when the oxygen coverage is greater than or equal to 0.362 ML (monolayer) and less than 1.0 ML. We therefore suggested that the surface oxygen stabilizes the top Co layer, thus preventing the substrate Cu atoms from migrating to the surface to form Cu/Co which is the lowest free energy state for the system in the absence of oxygen. Similarly, the addition of oxygen can also selectively pull Co atoms trapped in subsurface Cu layers to the surface which reduces intermixing in the Co on Cu interfaces. This is largely the result of the fact that the Co-O bond is stronger than that of Cu-O bond. For instance, at oxygen coverage of 0.33 ML, the binding energy for O on Co(0001) is 0.86 eV stronger than that for O on Cu(111). (unpublished²²)

In Co/Cu multilayers for GMR, both Co-on-Cu and Cu-on-Co interfaces exist. The addition of oxygen to stabilize the Co-on-Cu interface might be detrimental if the oxygen meets the Cu-on-Co interface, since it could promote intermixing of this interface. Herein we performed a series of *ab initio* density functional theory calculations for a range of different $\text{Cu}_x\text{Co}_{1-x}/\text{Co}(0001)$ intermixed (alloyed) and non-mixed interfaces in both the presence and absence of oxygen. We explicitly examined the influence of oxygen on the interfacial stability of Co and Cu alloys on Co(0001) over the range of oxygen coverage between 0.0 to 1.0 ML. We find that the nonmixed Co-on-Cu interface remains the most stable interface for oxygen coverage of less than 0.362 ML. Higher oxygen coverages favor intermixing at the Cu on Co interface. The addition of oxygen also influences the magnetic properties of the surface layers.

II. COMPUTATION DETAILS

All of the calculations reported herein were performed using periodic plane-wave density functional theory.^{23,24} as implemented in the Vienna *ab initio* Simulation Package (VASP).^{25,26} Nonlocal corrections to the exchange and correlation energies were evaluated using the Perdew-Wang 91 generalized gradient (GGA) approximation.²⁷ The electron-ion interactions were described by ultrasoft Vanderbilt pseudopotentials.²⁸ A plane wave cutoff energy of 396 eV was used in all the calculations. All the calculations were performed using spin-polarized calculations since Co is ferromagnetic and the differences in the spin-dependent scattering ultimately dictate GMR behavior.

C) Ordered
 $\text{Co}_{1\text{ML}}/\text{Cu}_{1\text{ML}}/\text{Co}(0001)$

The Cu/Co(0001) surface was simulated using a five-layer metal slab. The metal slab is repeated periodically in three dimensions and separated by a 10 Å vacuum region in the *z* (thickness) direction. The thickness of the vacuum region was systematically increased to ensure that the vacuum was large enough to avoid slab-slab interactions. Oxygen atoms were adsorbed onto one side of the Cu/Co(0001) slab. The metal atoms in the bottom two Co layers of the metal slab were fixed at their bulk lattice positions ($a=b=2.50$ Å and $c=4.05$ Å),^{22,29} while the adsorbed oxygen atoms and the atoms in the top three layers were allowed to relax. In evaluating the mixed $\text{Co}_x\text{Cu}_{1-x}/\text{Co}_{1-x}\text{Cu}_x/\text{Co}(0001)$ systems the same size and shape unit cells were used for different values of *x* in order to keep the same basis sets in determining the wave function for each system.

The influence of oxygen on the stability of various different Cu/Co compositions in the first two layers of the Cu/Co(0001) system was studied by preadsorbing 0.17, 0.33, 0.50, 0.67, 0.83, and 1.0 ML of atomic oxygen. The 0.33, 0.67, and 1.0 ML oxygen coverages were calculated by using the $(\sqrt{3} \times \sqrt{3}) R-30^\circ$ surface unit cell with one, two and three oxygen atoms, respectively. The 0.17 and 0.83 ML oxygen coverages were calculated using a (2×3) surface unit cell containing one and five oxygen atom(s), respectively. The 0.50 ML oxygen coverage was calculated with (2×2) unit surface cell containing one oxygen atom. The first Brillouin zones for all of the above surfaces were sampled with equivalent special *k* points in order to improve the accuracy of the calculations. In particular, the $5 \times 5 \times 1$, $5 \times 3 \times 1$ and $5 \times 5 \times 1$ Monkhorst-Pack *k*-point grids were used for the $(\sqrt{3} \times \sqrt{3}) R-30^\circ$, (2×3) and (2×2) , unit cells, respectively.

III. STABILITY OF THE Cu/Co(0001) SYSTEMS IN THE ABSENCE OF OXYGEN

The relative stability of the Cu and $\text{Cu}_x\text{Co}_{1-x}$ alloy surfaces on the Co(0001) substrate (where $x=0.0, 0.33, 0.67$, and 1.0) were examined first in the absence of oxygen. The nonmixed $\text{Cu}_{1\text{ML}}/\text{Co}_{1\text{ML}}/\text{Co}(0001)$ interface is a chemically abrupt interface consisting of a pure pseudomorphic overlayer of Cu on a Co(0001) substrate [Fig. 1(a)]. If copper is deposited onto a cobalt surface with high velocity it can exchange with surface Co atoms to create a random intermixed (alloy) layer at the interface, Fig. 1(b). In principle

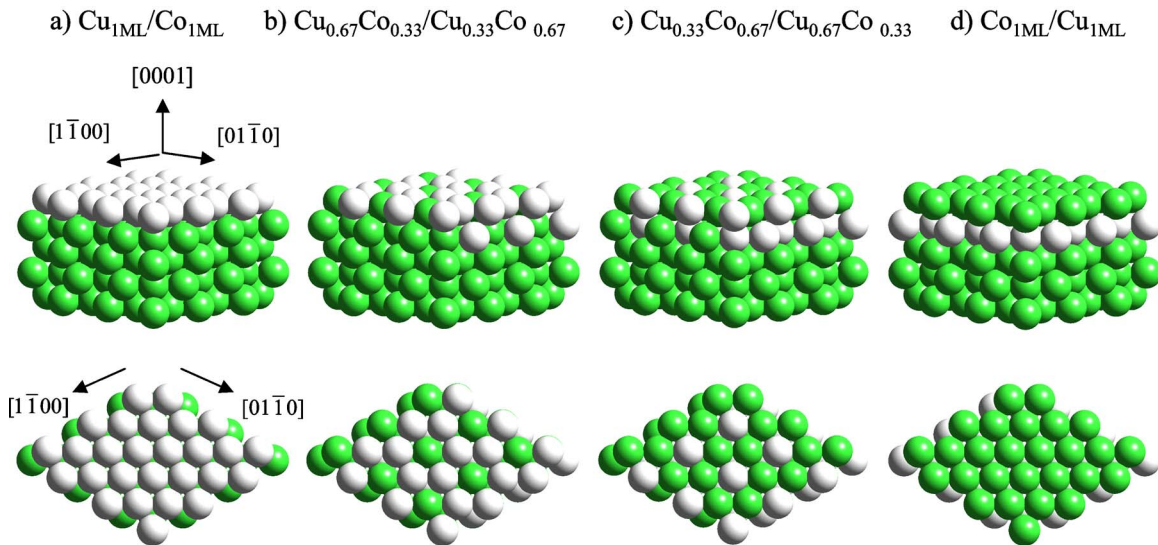


FIG. 2. (Color online) Side and top views of the various Cu/Co(0001) systems: (a) the nonmixed $\text{Cu}_1 \text{ML}/\text{Co}_1 \text{ML}/\text{Co}(0001)$ system, (b) the alloy-mixed $\text{Co}_{0.33}\text{Cu}_{0.67}/\text{Co}_{0.67}\text{Co}_{0.33}/\text{Co}(0001)$ system, (c) the alloy-mixed $\text{Co}_{0.67}\text{Cu}_{0.33}/\text{Co}_{0.33}\text{Cu}_{0.67}/\text{Co}(0001)$ system, and (d) the Co-capped $\text{Co}_1 \text{ML}/\text{Cu}_1 \text{ML}/\text{Co}(0001)$ systems. The top panels are the side views and the bottom panels are the top views. The light green spheres refer to the Co atoms whereas the white spheres refer to Cu atoms.

a Co capped $\text{Co}_1 \text{ML}/\text{Cu}_1 \text{ML}/\text{Co}(0001)$ fully intermixed interface, Fig. 1(c), can also be created. The interfaces constructed here maintain the same total number of Co and Cu atoms in the top two layers and were created by a simple exchange of one atom type for another while using supercells of the same shape and size for the studied $\text{Co}_x\text{Cu}_{1-x}/\text{Co}_{1-x}\text{Cu}_x/\text{Co}(0001)$ system (where $x=0.0, 0.33, 0.67,$ and 1.0). For the $x=0.33$ example, the $\text{Cu}_{0.33}\text{Co}_{0.67}/\text{Cu}_{0.67}\text{Co}_{0.33}/\text{Co}(0001)$ surface is one in which 67% of the original Cu atoms at the surface have been exchanged with Co atoms from the second layer. The specific systems examined are shown in Fig. 2. They consisted of (1) the nonmixed $\text{Cu}_1 \text{ML}/\text{Co}_1 \text{ML}/\text{Co}(0001)$ surface [Fig. 2(a)]; (2) the mixed $\text{Co}_{0.33}\text{Cu}_{0.67}/\text{Co}_{0.67}\text{Cu}_{0.33}/\text{Co}(0001)$ surface alloy [Fig. 2(b)] and the mixed $\text{Co}_{0.67}\text{Cu}_{0.33}/\text{Co}_{0.33}\text{Cu}_{0.67}/\text{Co}(0001)$ surface alloy [Fig. 2(c)]; (3) the capped $\text{Co}_1 \text{ML}/\text{Cu}_1 \text{ML}/\text{Co}(0001)$ fully mixed system with 1 ML Co capping the top of the $\text{Cu}/\text{Co}(0001)$ surface [Fig. 2(d)].

In order to analyze the stability of these different surfaces, we compared their surface formation energies. The surface formation energy, $E_{f,top_surface}$ here refers to the energy to create the top surface from its bulk atomic constituents and is computed as:

$$E_{f,top_surface} = \frac{1}{N_b} \underbrace{(E_{slab} - N_{\text{Cu}}E_{\text{Cu}}^{\text{bulk}} - N_{\text{Co}}E_{\text{Co}}^{\text{bulk}})}_{\text{First term}} - \underbrace{E_{f,\text{Co}(0001)}}_{\text{Last term}} \quad (1)$$

where N_b is one half of the total number of surface atoms (including both the top and bottom surfaces) per unit cell, E_{slab} is the total energy of the slab, N_{Cu} and N_{Co} are the

number of Cu and Co atoms in the slab and $E_{\text{Cu}}^{\text{bulk}}$ and $E_{\text{Co}}^{\text{bulk}}$ are the energies for the Cu and the Co atom in the respective bulk crystals at their theoretically calculated equilibrium lattice constants. The first term in Eq. (1) refers to the formation energy for the top and the bottom surfaces together. The last term in Eq. (1) refers to the energy to create the bottom Co surface, which was calculated to be 0.69 (eV/atom) according to this same equation with the exception that the number of Cu atoms is zero. Subtracting the first and second terms provides the formation energy for the top surface. For reference, a positive formation energy implies that the formation of the CoCu surface from its constituent atoms taken from bulk fcc Cu and hcp Co metals requires energy and is therefore endothermic.^{22,29} Lower formation energies correspond to more stable surfaces. For comparison purposes, we reference the surface energies for each system to the surface energy of the $\text{Cu}_1 \text{ML}/\text{Co}_1 \text{ML}/\text{Co}(0001)$ system to define referenced energies (ΔET).

The results for the energies of the bare surfaces are presented in Table I. They indicate that the nonmixed $\text{Cu}_1 \text{ML}/\text{Co}_1 \text{ML}/\text{Co}(0001)$ system [Fig. 2(a)] has the lowest formation energy, 0.49 eV/atom, thus making it the most stable surface. The Co-capped $\text{Co}_1 \text{ML}/\text{Cu}_1 \text{ML}/\text{Co}(0001)$ system [Fig. 2(d)] is the least stable surface. It requires an extra 0.48 eV/atom energy to form as compared with the nonmixed $\text{Cu}_1 \text{ML}/\text{Co}_1 \text{ML}/\text{Co}(0001)$ system. The mixed $\text{Co}_{0.33}\text{Cu}_{0.67}/\text{Co}_{0.67}\text{Cu}_{0.33}/\text{Co}(0001)$ and $\text{Co}_{0.67}\text{Cu}_{0.33}/\text{Co}_{0.33}\text{Cu}_{0.67}/\text{Co}(0001)$ alloy surfaces are metastable, with energies that are 0.22 and 0.40 eV/atom higher than the nonmixed $\text{Cu}_1 \text{ML}/\text{Co}_1 \text{ML}/\text{Co}(0001)$ surface (see Table I). The results presented in Table I indicate there is essentially no driving force for intermixing for the clean $\text{Cu}_1 \text{ML}/\text{Co}(0001)$ surface.

Further analysis of the results suggests that there is a correlation between the concentration of the surface Cu atoms

TABLE I. The formation energy, E_f , in eV/atom and the total energy difference, ΔE_T , in eV/atom for different Cu/Co(0001) systems. ΔE_T is calculated by subtracting the total energy of a system from that of the reference system. The reference surface is defined here as the nonmixed $\text{Cu}_1 \text{ML}/\text{Co}_1 \text{ML}/\text{Co}(0001)$ system [shown in Fig. 1(a)].

System	E_f (eV/atom)	ΔE_T (eV/atom)
$\text{Cu}_1 \text{ML}/\text{Co}_1 \text{ML}/\text{Co}(0001)$	0.49	0.00
$\text{Co}_{.33}\text{Cu}_{.67}/\text{Co}_{.67}\text{Cu}_{.33}/\text{Co}(0001)$	0.71	0.22
$\text{Co}_{.67}\text{Cu}_{.33}/\text{Co}_{.33}\text{Cu}_{.67}/\text{Co}(0001)$	0.89	0.40
$\text{Co}_1 \text{ML}/\text{Cu}_1 \text{ML}/\text{Co}(0001)$	0.97	0.48

and the formation energy. The higher the concentration of Cu in the surface layer, the lower the formation energy. In other words, Cu atoms prefer to reside at the surface. One of the critical driving forces for the segregation of Cu to the surface is the difference between the surface energies for Cu and Co, which are, 1.9 and 2.7 J/m², respectively.^{30,31} A Copper also has a larger radius and therefore prefers to segregate out to the surface to reduce the lattice strain energy and increase the entropy and lower the overall free energy. This is reflected by the fact that the interlayer distances between the first two surface layers, d_{12} , (Fig. 3) in all of the Cu/Co(0001) surfaces expand from about 1.97 Å to 2.11 Å (see Table II). Therefore, intermixing is minimized when Cu is deposited on Co to form the Co-on-Cu interface. As might be expected, the opposite result is true for the Co-on-Cu interface

TABLE II. DFT calculated structural parameters (d_{01} , d_{12} , and d_{23}) in Å for the various studied surfaces at oxygen coverage from 0.0 to 1.0 monolayer (ML). d_{01} refers to the average height of the adsorbed oxygen atom. d_{12} and d_{23} are the average first and second interlayer distances, where the center of mass of the layer is used. The bulk interlayer distances of the Co(0001) and Cu(111) are 2.03 Å and 2.11 Å, respectively.

Surfaces	Binding site	d_{01} (Å)				d_{12} (Å)				d_{23} (Å)			
		Oxygen coverage (ML)				Oxygen coverage (ML)				Oxygen coverage (ML)			
		0.33	0.67	1.00	0.00	0.33	0.67	1.00	0.00	0.33	0.67	1.00	
$\text{Co}_1 \text{ML}/\text{Cu}_1 \text{ML}/\text{Co}(0001)$	hcp	1.18	1.08	1.05	2.12	2.12	2.16	2.17	2.12	2.12	2.18	2.17	
	fcc	1.18	1.07	1.05	2.12	2.12	2.17	2.17	2.12	2.12	2.17	2.18	
Co(0001)	hcp	1.17	1.11	1.06	1.97	2.01	2.04	2.13	2.05	2.03	2.02	1.99	
	fcc	1.19	1.11	1.06	1.97	2.02	2.08	2.15	2.05	2.02	1.99	1.98	
	hcp	1.99 ± 0.02^a				2.06 ± 0.04^a							
$\text{Co}_{0.67}\text{Cu}_{0.33}/\text{Co}_{0.33}\text{Cu}_{0.67}/\text{Co}(0001)$	hcp	1.21	1.14	1.11	2.10	2.10	2.13	2.18	2.08	2.06	2.05	2.04	
	fcc	1.20	1.13	1.11	2.10	2.09	2.13	2.17	2.08	2.07	2.06	2.05	
$\text{Co}_{0.33}\text{Cu}_{0.67}/\text{Co}_{0.67}\text{Cu}_{0.33}/\text{Co}(0001)$	hcp	1.21	1.18	1.20	2.09	2.13	2.17	2.23	2.03	2.04	2.03	2.02	
	fcc	1.21	1.17	1.19	2.09	2.10	2.15	2.24	2.03	2.06	2.04	2.02	
Cu(111)	hcp	1.18	1.09	1.16	2.08	2.11	2.15	2.15	2.12	2.11	2.10	2.09	
	fcc	1.16	1.07	1.16	2.08	2.10	2.10	2.14	2.12	2.11	2.10	2.10	
	fcc	2.07 ± 0.01^a				2.08 ± 0.02^a							
$\text{Cu}_1 \text{ML}/\text{Co}_1 \text{ML}/\text{Co}(0001)$	hcp	1.25	1.20	1.30	2.11	2.17	2.21	2.21	1.96	1.99	2.00	1.98	
	fcc	1.22	1.19	1.30	2.11	2.15	2.20	2.20	1.96	1.99	2.00	1.98	

^aStructure parameters derived by LEED analysis by Prieto *et al.* (Ref. 45).

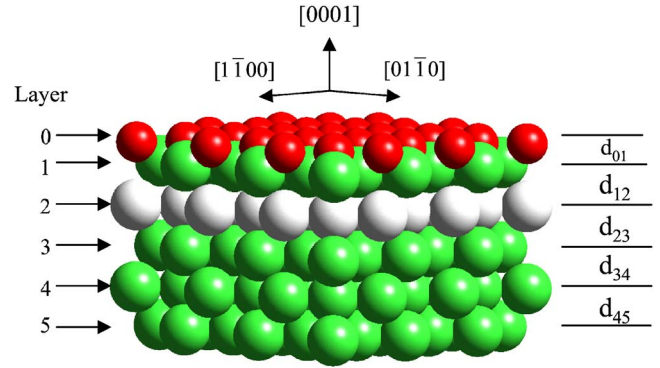


FIG. 3. (Color online) Side view of the O/Co₁ ML/Cu₁ ML/Co(0001) surface. d_{01} is the average vertical height of the adsorbed atomic oxygen atom. d_{12} , d_{23} , d_{34} , and d_{45} are the average first, second, third, and fourth interlayer distances, where the center of mass of each layer is used to calculate the distances. Co, Cu, and O atoms are represented by light green, white, and small red spheres, respectively.

whereby intermixing will much more likely occur thus increasing the concentration of Cu in the surface alloy. These results are in good agreement with experiments,^{8,10,32,33} as well as with other theoretical calculations,¹⁵ i.e., that intermixing occurs predominantly at Co/Cu(111) surface, which is observed much more often in the experiments.^{8,10,32,33}

IV. OXYGEN BINDING

The presence of oxygen can significantly alter the stability of different interfaces examined above. As was discussed,

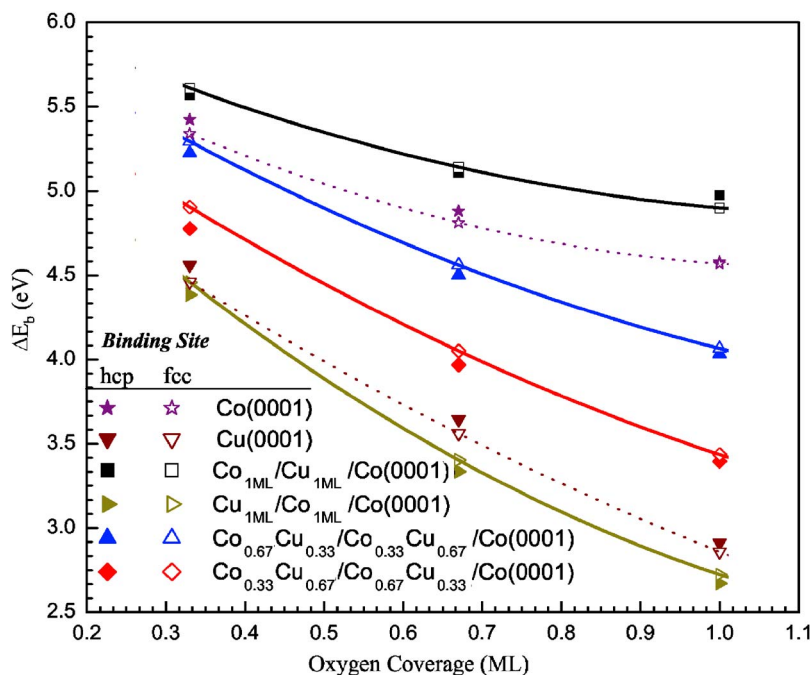


FIG. 4. (Color online) The correlation between the binding energy, E_b , in eV/atom of an adsorbed oxygen atom and the surface atomic oxygen coverage. E_b is calculated with respect to the gas-phase atomic oxygen and the bare metal slab. The oxygen coverage is varied between 0.33 ML to 1.00 ML. Two types of binding sites were considered: the fcc hollow site shown by the open interior symbol and the hcp hollow site indicated by the solid interior symbol.

oxygen binds more strongly to Co than to Cu. The relative binding energies for oxygen to the Co and Cu atoms in a Co-Cu alloy is likely to be an important factor in determining the stability of the surface structure. We have calculated the binding energies for atomic oxygen on the same Cu/Co surfaces discussed above for oxygen surface coverages between 0.0 and 1.0 ML. The binding energy (E_b) we report is defined as the energy released upon the adsorption of an oxygen atom. A positive value indicates that the adsorption of an oxygen atom is stable on the surface.²² The binding energies for atomic oxygen on the various different Cu/Co(0001) surfaces identified above are plotted as a function of coverage in Fig. 4. The binding energies for atomic oxygen on the Co(0001) and Cu(111) surfaces were also included for comparison.

Oxygen binds strongly to all of the metal surfaces examined from a low of 2.67 eV/atom to a high of 5.74 eV/atom (Table III and Fig. 4). This is expected since atomic oxygen itself is not stable in the gas phase. The results in Fig. 4 indicate that atomic oxygen is most strongly bound at the three-fold fcc sites for most of the surfaces examined, including Cu(111), nonmixed Cu1 ML/Co(0001), Co-capped Co1 ML/Cu1 ML/Co(0001) and mixed alloy $\text{Cu}_x\text{Co}_{1-x}/\text{Cu}_{1-x}\text{Co}_x/\text{Co}(0001)$. In all cases, the oxygen binding energy decreases with increasing oxygen coverage. This is due to the lateral repulsive interactions between the adsorbed oxygen atoms that arise from through surface and through-space electrostatic repulsion. Pauli repulsion between filled states tends to dominate the energy. The repulsive interactions increase substantially as the oxygen atoms begin to share metal atoms. This same trend has also been observed on several other metal surfaces, including O/Ag(111),³⁴ O/Rh(111),³⁵ O/Ru(0001),³⁶ O/Co/Cu(111),²² and O/Cu/Co/Cu(111)²²

The binding energy of oxygen on the metal is predominantly determined by the nature of the specific metal atoms

to which it is bound. For example, the binding energy of oxygen on the Co(0001) surface at low surface coverages (~ 0.33 ML) is nearly 1.0 eV/atom stronger than that for oxygen on the Cu(111) surface. The significantly weaker bonding to Cu is attributed to the greater Pauli repulsion between the electrons on oxygen and the nearly filled d band of Cu. The difference in the oxygen binding energy on Co(0001) and Cu(111) increases significantly with increases in the oxygen surface coverage. At full monolayer coverage, the binding energy for oxygen on Co(0001) is 1.67 eV/atom stronger than that on Cu(111). The large differences between Co and Cu are primarily a consequence of the substantial increase in Pauli repulsion between lone pairs of electrons on oxygen and the electrons at the top of the valence band of the metal. The binding energy for oxygen therefore increases with an increase in the number of Co atoms in the surface. Figure 4 shows that at the same oxygen coverage, the binding energies for atomic oxygen decrease in the following order:

$$\begin{aligned}
 & \text{Co}_{1\text{ ML}}/\text{Cu}_{1\text{ ML}}/\text{Co}(0001) \\
 & > \text{Co}(0001) > \text{Co}_{0.67}\text{Cu}_{0.33}/\text{Co}_{0.33}\text{Cu}_{0.67}/\text{Co}(0001) \\
 & > \text{Co}_{0.33}\text{Cu}_{0.67}/\text{Co}_{0.67}\text{Cu}_{0.33}/\text{Co}(0001) \\
 & > \text{Cu}_{1\text{ ML}}/\text{Co}_{1\text{ ML}}/\text{Cu}(111) > \text{Cu}(111) \\
 & > \text{Cu}_{1\text{ ML}}/\text{Co}_{1\text{ ML}}/\text{Co}(0001).
 \end{aligned}$$

The adsorption energies can also change as the result of more subtle electronic changes that occur with changes in the next-nearest neighbor metal atoms or from changes to lattice spacing as the result of changes to the bottom substrate. Electronic effects occur when there are changes in the composition of the first few layers of the slab which affect the binding of oxygen to the same constituent atoms. This can occur when as a result of changes in the degree of charge

TABLE III. Calculated binding energy, E_b , in eV/atom for a surface oxygen atom at the hcp site or the fcc site, and the difference in binding energy, $\Delta E_{b,fcc \rightarrow hcp}$, in eV/atom. E_b is calculated with respect to the gas-phase oxygen atom and the bare metal slab. The difference in binding energies is reported as $\Delta E_{b,fcc \rightarrow hcp} = E_{b,hcp} - E_{b,fcc}$, where $E_{b,hcp}$ and $E_{b,fcc}$ refer to the binding energy of a surface oxygen atom at the hcp and fcc sites respectively. A negative value of $\Delta E_{b,fcc \rightarrow hcp}$ indicates that oxygen prefers to adsorb at the fcc site.

Surfaces	E_b (eV)						
	Binding Site	Oxygen Coverage			$\Delta E_{b,fcc \rightarrow hcp}$ (eV/atom)		
		0.33	0.67	1.00			
$\text{Co}_1 \text{ ML}/\text{Cu}_1 \text{ ML}/\text{Cu}(111)^a$	fcc	5.74	5.20	5.13			
$\text{Co}_1 \text{ ML}/\text{Cu}_1 \text{ ML}/\text{Co}(0001)$	hcp	5.57	5.11	4.98	-0.04	-0.03	0.08
	fcc	5.61	5.14	4.90			
$\text{Co}(0001)$	hcp ^a	5.42	4.88	4.58	0.08	0.07	0.01
	fcc	5.34	4.81	4.57			
$\text{Co}_{0.67}\text{Cu}_{0.33}/\text{Co}_{0.33}\text{Cu}_{0.67}/\text{Co}(0001)$	hcp	5.22	4.50	4.03	-0.07	-0.06	-0.03
	fcc	5.29	4.56	4.07			
$\text{Co}_{0.33}\text{Cu}_{0.67}/\text{Co}_{0.67}\text{Cu}_{0.33}/\text{Co}(0001)$	hcp	4.78	3.97	3.40	-0.13	-0.08	-0.04
	fcc	4.91	4.05	3.44			
$\text{Cu}_1 \text{ ML}/\text{Co}_1 \text{ ML}/\text{Cu}(111)^a$	fcc	4.63	3.61	2.94			
$\text{Cu}(111)$	hcp	4.46	3.56	2.86	-0.10	-0.08	-0.05
	fcc ^a	4.56	3.64	2.91			
$\text{Cu}_1 \text{ ML}/\text{Co}_1 \text{ ML}/\text{Co}(0001)$	hcp	4.38	3.34	2.67	-0.07	-0.07	-0.05
	fcc	4.46	3.40	2.72			

^aH Wen, M. Neurock, and H. N. Wadley (Ref. 22).

transfer or orbital overlap to the same central Co (or Cu) atom from changes in the specific neighboring atoms. Alternatively, these changes can be the result of structural changes in the underlying lattice. For example, the binding energy for oxygen on the $\text{Co}_1 \text{ ML}/\text{Cu}_1 \text{ ML}/\text{Co}(0001)$ surface is stronger than that on the pure $\text{Co}(0001)$ surface. Substituting Cu for Co in the second layer increases the surface Co's ability to adsorb oxygen. Since the substrate for both surfaces is $\text{Co}(0001)$, changes here are more likely the result of changes in the electronic structure of the surface Co atoms as the result of changes in composition of the second layer. The interaction between oxygen and Co is controlled by the coupling to d states near the Fermi level and can be readily understood by the d -band center model proposed by Hammer and Nørskov.³⁷ Subsurface Cu shifts the center of the d -band closer to the Fermi level. This enhances the interaction between oxygen and the Co surface, and increases orbital overlap which thus increases the binding energy. This can also be understood in terms of bond order conservation. The Co-Co bond is stronger than the Co-Cu bond. The Co surface atoms in the $\text{Co}/\text{Cu}_1 \text{ ML}/\text{Co}(0001)$ have a lower bond order than the Co surface atoms on the $\text{Co}(0001)$ substrate. To compensate for the lower bond order, the $\text{Co}/\text{Cu}_1 \text{ ML}/\text{Co}(0001)$ system binds more strongly to the oxygen.

Previously we reported on calculations for oxygen on the $\text{Cu}(111)$ substrate.³⁸ Some of the binding energy results are also included in Table III for comparison. The substitution of

Co for Cu [$\text{Cu}_1 \text{ ML}/\text{Co}_1 \text{ ML}/\text{Cu}(111)$] in the subsurface layer does not appear to appreciably change the binding energy of oxygen. The Cu surface states which are nearly filled dominate. There is very little change in the filling of these states when the subsurface layer is changed to Co. The adsorption energies for oxygen on $\text{Cu}_1 \text{ ML}/\text{Co}_1 \text{ ML}/\text{Cu}(111)$ and oxygen on $\text{Cu}(111)$ are quite similar. The oxygen binding energies are therefore within 0.05 eV of one another for all oxygen coverages.

Finally we explore how changes in the metal substrate that are removed from the surface can influence the oxygen binding energy. The first two layers for the $\text{Cu}_1 \text{ ML}/\text{Co}_1 \text{ ML}/\text{Cu}(111)$ and $\text{Cu}_1 \text{ ML}/\text{Co}_1 \text{ ML}/\text{Co}(0001)$ surfaces are identical. The former, however, is supported on a $\text{Cu}(111)$ substrate whereas the latter is supported on a $\text{Co}(0001)$ substrate. In the $\text{Cu}_1 \text{ ML}/\text{Co}_1 \text{ ML}/\text{Cu}(111)$ surface there is a lattice expansion of the Co layer that results from the lattice mismatch of the Co on $\text{Cu}(111)$. This ultimately propagates to the surface thus resulting in a somewhat stronger oxygen on the $\text{Cu}_1 \text{ ML}/\text{Co}_1 \text{ ML}/\text{Cu}(111)$ surface over the $\text{Cu}_1 \text{ ML}/\text{Co}_1 \text{ ML}/\text{Co}(0001)$ surface. This is seen in the resulting oxygen binding energies reported for these two surfaces in Table III. In comparing the results for $\text{Cu}_1 \text{ ML}/\text{Co}_1 \text{ ML}/\text{Cu}(111)$, $\text{Cu}_1 \text{ ML}/\text{Co}_1 \text{ ML}/\text{Co}(0001)$ and $\text{Cu}(111)$, we note that while there are differences in these three systems, the differences in the calculated oxygen binding energies are rather small.

For each of the surfaces considered, we examined oxygen

binding at both the *fcc* and the *hcp* threefold surface sites. The structural changes for oxygen adsorbed at these two different sites were found to be quite small as is seen in Table II. The corresponding difference between the binding energies for oxygen at the *fcc* and *hcp* sites, $\Delta E_{b, fcc \rightarrow hcp}$, reported in Table III were also rather small, and in the range from 0.01 to 0.13 eV/atom which is only 0–3 % of the actual binding energy. A negative value for $\Delta E_{b, fcc \rightarrow hcp}$ indicates that the oxygen at the *fcc* binding site is more favorable, whereas a positive value of $\Delta E_{b, fcc \rightarrow hcp}$ suggests that the oxygen at the *hcp* binding site is more favorable. Oxygen slightly prefers to sit at the *fcc* site on all the four Cu/Co(0001) surfaces as well as the homogenous Cu(111) surface for oxygen coverage up to 1.0 ML. In contrast, oxygen prefers the *hcp* site on the homogenous Co(0001) surface. The surface or subsurface Cu layer in the Cu/Co(0001) system, therefore, influences the preference for the oxygen binding site. This influence, nonetheless, can be suppressed when the interaction of surface Co and the adsorbed oxygen coverage is large enough, such as the case for 1.0 ML in the $\text{Co}_1 \text{ ML}/\text{Cu}_1 \text{ ML}/\text{Co}(0001)$ system due to the strength of the Co-O interaction.

V. STABILITY OF THE VARIOUS Cu/Co(0001) SURFACES IN THE PRESENCE OF OXYGEN

The binding energies of oxygen provide a measure of the strength of the metal-oxygen bond on each of the surfaces examined and help to rationalize the stability of different surfaces exposed to oxygen. Which surface is most stable in the presence of oxygen, however, requires a comparison of the total energy for a specific surface with oxygen against some reference ground state surface with oxygen. The relative stability is defined here as, ΔE_T ,²² which is the energy difference between the surface of interest and the nonmixed $\text{Cu}_1 \text{ ML}/\text{Co}_1 \text{ ML}/\text{Co}(0001)$ surface structure, chosen here as the reference system. Both surfaces have identical amounts of oxygen adsorbed. A positive ΔE_T implies that the system of interest is less stable than the nonmixed $\text{Cu}_1 \text{ ML}/\text{Co}_1 \text{ ML}/\text{Co}(0001)$ reference surface, whereas a negative value of ΔE_T implies that the reference surface is more stable.

The stability of the nonmixed $\text{Cu}_1 \text{ ML}/\text{Co}_1 \text{ ML}/\text{Co}(0001)$ and the Co-capped $\text{Co}_1 \text{ ML}/\text{Cu}_1 \text{ ML}/\text{Co}(0001)$ are the two end points and therefore were examined first. ΔE_T was calculated for $\text{Cu}_1 \text{ ML}/\text{Co}_1 \text{ ML}/\text{Co}(0001)$ and $\text{Co}_1 \text{ ML}/\text{Cu}_1 \text{ ML}/\text{Co}(0001)$ at the oxygen coverage of 0.0, 0.17, 0.33, 0.50, 0.67, 0.83, and 1.0 ML. As seen in Fig. 5, the value of ΔE_T for the capped $\text{Co}_1 \text{ ML}/\text{Cu}_1 \text{ ML}/\text{Co}(0001)$ continues to decrease with increasing oxygen coverage. This implies that the addition of oxygen helps to eventually stabilize the Co-capped $\text{Co}_1 \text{ ML}/\text{Cu}_1 \text{ ML}/\text{Co}(0001)$ surface just as it was found to stabilize the $\text{Co}_1 \text{ ML}/\text{Cu}_1 \text{ ML}/\text{Cu}(111)$ (Ref. 22) surface. This is the result of the strong bonding between the surface Co atoms and the adsorbed oxygen atoms.

It is important to note that the two curves for the mixed $\text{Co}_1 \text{ ML}/\text{Cu}_1 \text{ ML}/\text{Co}(0001)$ and the nonmixed $\text{Cu}_1 \text{ ML}/$

$\text{Co}_1 \text{ ML}/\text{Co}(0001)$ surfaces cross at the oxygen coverage of 0.362 ML (Fig. 5). For oxygen coverages less than 0.362 ML, the value of ΔE_T for the capped (mixed) $\text{Co}_1 \text{ ML}/\text{Cu}_1 \text{ ML}/\text{Co}(0001)$ is positive and larger than that of the nonmixed $\text{Cu}_1 \text{ ML}/\text{Co}_1 \text{ ML}/\text{Co}(0001)$. This suggests that the nonmixed $\text{Cu}_1 \text{ ML}/\text{Co}_1 \text{ ML}/\text{Co}(0001)$ is more stable than the capped $\text{Co}_1 \text{ ML}/\text{Cu}_1 \text{ ML}/\text{Co}(0001)$ surface at oxygen coverage less than 0.362 ML. In contrast, at oxygen coverages greater than 0.362 ML, the value for ΔE_T for the capped $\text{Co}_1 \text{ ML}/\text{Cu}_1 \text{ ML}/\text{Co}(0001)$ surface is negative and thus less than that for the nonmixed $\text{Cu}_1 \text{ ML}/\text{Co}_1 \text{ ML}/\text{Co}(0001)$. This suggests that the capped (mixed) $\text{Co}_1 \text{ ML}/\text{Cu}_1 \text{ ML}/\text{Co}(0001)$ is now more stable than the nonmixed $\text{Cu}_1 \text{ ML}/\text{Co}_1 \text{ ML}/\text{Co}(0001)$, and that intermixing occurs for the $\text{Cu}_1 \text{ ML}/\text{Co}(0001)$ systems when the oxygen coverage is higher than 0.362 ML.

For oxygen coverages greater than 0.45 ML, the curves in Fig. 5 reveal a systematic ordering with Co content whereby the surfaces with the highest composition of Co show the greatest stability. The stability of these surfaces above 0.45 ML of oxygen is as follows:

$$\begin{aligned} \text{Co}_1 \text{ ML}/\text{Cu}_1 \text{ ML}/ &> \text{Co}_{0.667}\text{Cu}_{0.33}/\text{Co}_{0.33}\text{Cu}_{0.67}/ \\ &> \text{Co}_{0.33}\text{Cu}_{0.67}/\text{Co}_{0.67}\text{Cu}_{0.33}/ \\ &> \text{Cu}_1 \text{ ML}/\text{Co}_1 \text{ ML}/. \end{aligned}$$

The energy difference between each of these increases with increasing oxygen coverages. This indicates that there is an increase in the stability for surfaces which contain higher compositions of Co. Intermixing appears to be favored when the surface coverage of oxygen exceeds 0.362 ML. In order to prevent intermixing, the oxygen coverage in the $\text{Cu}_1 \text{ ML}/\text{Co}_1 \text{ ML}/\text{Co}(0001)$ system should therefore be kept below 0.362 ML.

In addition to the pseudomorphic overlayers discussed above, we have also analyzed the stability of the mixed $\text{Cu}_x\text{Co}_{(1-x)}/\text{Cu}_{(1-x)}\text{Co}_x/\text{Co}(0001)$ alloy surfaces as well. The relative stability, ΔE_T , for the mixed $\text{Co}_{0.67}\text{Cu}_{0.33}/\text{Co}_{0.33}\text{Cu}_{0.67}/\text{Co}(0001)$ and $\text{Co}_{0.33}\text{Cu}_{0.67}/\text{Co}_{0.67}\text{Cu}_{0.33}/\text{Co}(0001)$ surface alloys were calculated at different oxygen coverage. The results are shown in Fig. 5. The curves for both of these mixed alloy surfaces decrease with increasing oxygen coverage just as the results from the capped $\text{Co}_1 \text{ ML}/\text{Cu}_1 \text{ ML}/\text{Co}(0001)$ did. Surface oxygen stabilizes these two alloy-mixed Cu/Co(0001) surfaces.

The stabilization of Co over Cu at the surface also increases with increasing oxygen coverage. The stabilization effect induced by the adsorbed oxygen increases with an increase in the concentration of surface Co atoms. This stabilization can also be attributed to the stronger interaction between adsorbed oxygen and surface Co atoms than between the adsorbed oxygen and surface Cu atoms. On the other hand, the curves for the $\text{Co}_{0.67}\text{Cu}_{0.33}/\text{Co}_{0.33}\text{Cu}_{0.67}/\text{Co}(0001)$ and the $\text{Co}_{0.33}\text{Cu}_{0.67}/\text{Co}_{0.67}\text{Cu}_{0.33}/\text{Co}(0001)$ surfaces cross the horizontal line [which corresponds to the

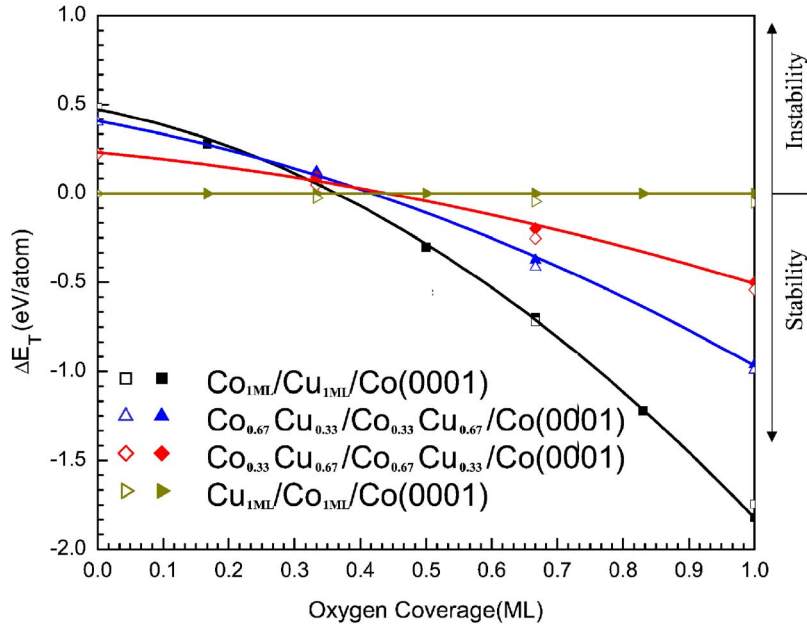


FIG. 5. (Color online) The influence of the oxygen coverage on the difference in the total energy ($\Delta E_{T,0}$) for various mixed and nonmixed Cu/Co(0001) interfaces. The difference in the total energy between surfaces ($\Delta E_{T,0}$) is defined as the total energy ($E_{T,i}$) of the surface of interest minus that of the reference surface, that is, $\Delta E_{T,0} = E_{T,i} - E_{T,0}$. The reference surface used herein is the nonmixed $\text{Cu}_1 \text{ ML} / \text{Co}_1 \text{ ML} / \text{Co}(0001)$ surface. Two types of oxygen binding sites were considered: the hcp site (the symbol with a solid interior) and the fcc site (the symbol with an open interior).

$\text{Cu}_1 \text{ ML} / \text{Co}_1 \text{ ML} / \text{Co}(0001)$ system] at 0.418 ML and 0.439 ML, respectively (Fig. 5). This suggests that the nonmixed $\text{Cu}_1 \text{ ML} / \text{Co}_1 \text{ ML} / \text{Co}(0001)$ surface can transition into the $\text{Co}_{0.67}\text{Cu}_{0.33} / \text{Co}_{0.33}\text{Cu}_{0.67} / \text{Co}(0001)$ surface if the oxygen coverage is greater than 0.418 ML, and then into the $\text{Co}_{0.33}\text{Cu}_{0.67} / \text{Co}_{0.67}\text{Cu}_{0.33} / \text{Co}(0001)$ surface if oxygen coverage is greater than 0.439 ML. However, when the oxygen coverage exceeds 0.362 ML, the mixed $\text{Cu}_x\text{Co}_{(1-x)} / \text{Cu}_{(1-x)}\text{Co}_x / \text{Co}(0001)$ surface alloys are only metastable systems which may subsequently convert to the more stable capped $\text{Co}_1 \text{ ML} / \text{Cu}_1 \text{ ML} / \text{Co}(0001)$ system. This implies that the nonmixed $\text{Cu}_1 \text{ ML} / \text{Co}_1 \text{ ML} / \text{Co}(0001)$ surface, the mixed $\text{Co}_{0.67}\text{Cu}_{0.33} / \text{Co}_{0.33}\text{Cu}_{0.67} / \text{Co}(0001)$ and $\text{Co}_{0.33}\text{Cu}_{0.67} / \text{Co}_{0.67}\text{Cu}_{0.33} / \text{Co}(0001)$ alloy surfaces will convert to the capped $\text{Co}_1 \text{ ML} / \text{Cu}_1 \text{ ML} / \text{Co}(0001)$ if the oxygen coverage is

higher than 0.362 ML. In order to prevent this intermixing, the oxygen coverage, should be kept below the threshold oxygen coverage of 0.362 ML. Lower oxygen coverages lead to less intermixing. Higher coverages of oxygen may be necessary though to aid the Co/Cu(111) interface.

The effect of the oxygen coverage on the stability of the various $\text{Cu}_x\text{Co}_{(1-x)} / \text{Cu}_{(1-x)}\text{Co}_x / \text{Co}(0001)$ systems reported above were all carried out with oxygen adsorbed at the three-fold hcp site. The differences, however, in the stabilities for oxygen at the fcc and hcp sites on these surfaces however were found to be quite small and insignificant as seen in Fig. 5. The values for ΔE_T for the fcc-bound oxygen (the symbol with an open interior, Fig. 5) and the hcp-bound oxygen (the symbol with a solid interior, Fig. 5) are very close to one another. The energy difference induced by the different binding sites is not more than 0.08 eV/atom (Table

TABLE IV. Relative stability of the different Cu/Co interfaces for the Cu/Co(0001) system in the presence of 0.0, 0.33, 0.67, and 1.00 ML of atomically adsorbed oxygen. The relative stability is measured by ΔE_T , calculated by subtracting the total energy of the interested system from the system where oxygen is adsorbed at the hcp site. A negative ΔE_T indicates that the system with the fcc-site oxygen is more stable.

Surfaces	Oxygen Binding Site	ΔE_T (eV/atom)			
		Oxygen coverage (ML)			
		0.00	0.33	0.67	1.00
$\text{Co}_1 \text{ ML} / \text{Cu}_1 \text{ ML} / \text{Co}(0001)$	hcp	0.00	0.00	0.00	0.00
	fcc	0.00	-0.01	-0.02	0.08
$\text{Co}_{0.67}\text{Cu}_{0.33} / \text{Co}_{0.33}\text{Cu}_{0.67} / \text{Co}(0001)$	hcp	0.00	0.00	0.00	0.00
	fcc	0.00	-0.01	-0.01	-0.01
$\text{Co}_{0.33}\text{Cu}_{0.67} / \text{Co}_{0.67}\text{Cu}_{0.33} / \text{Co}(0001)$	hcp	0.00	0.00	0.00	0.00
	fcc	0.00	-0.01	-0.02	-0.01
$\text{Cu}_1 \text{ ML} / \text{Co}_1 \text{ ML} / \text{Co}(0001)$	hcp	0.00	0.00	0.00	0.00
	fcc	0.00	-0.02	-0.05	-0.05

TABLE V. The effects of oxygen adsorption and interlayer stacking on the stability of the nonmixed $\text{Cu}_1 \text{ ML}/\text{Co}_1 \text{ ML}/\text{Co}(0001)$ and the Co-capped (mixed) $\text{Co}_1 \text{ ML}/\text{Cu}_1 \text{ ML}/\text{Co}(0001)$ systems. Atomic oxygen coverage of 0.0, 0.33, 0.67, and 1.00 ML was explored, respectively. The relative stability is measured by ΔE_T , calculated by subtracting the total energy of the interested system from that of a reference system. The reference system is the hcp-stacking Cu/Co(0001) systems where atomic oxygen sits at the hcp site. A negative ΔE_T indicates that the system of interest is more stable than the reference system.

Surfaces	Oxygen Binding Site	Slab stacking pattern			Oxygen coverage (ML)			
		First layer	Second layer	Third–Fifth layer	0.00	0.33	0.67	1.00
					$\Delta E_T(\text{eV}/\text{atom})$			
$\text{Cu}_1 \text{ ML}/\text{Co}_1 \text{ ML}/\text{Co}(0001)$	hcp	hcp	hcp	hcp	0.00	0.00	0.00	0.00
	fcc	hcp	hcp	hcp	0.00	-0.02	-0.05	-0.05
	fcc	fcc	fcc	fcc	0.04	0.00	-0.01	0.00
	fcc	fcc	hcp	hcp	-0.01	-0.02	-0.05	-0.05
$\text{Co}_1 \text{ ML}/\text{Cu}_1 \text{ ML}/\text{Co}(0001)$	hcp	hcp	hcp	hcp	0.00	0.00	0.00	0.00
	fcc	hcp	hcp	hcp	0.00	-0.01	-0.02	0.08
	fcc	fcc	fcc	fcc	0.00	-0.01	-0.01	0.11
	hcp	hcp	fcc	hcp	-0.02	-0.01	-0.01	0.12
		fcc	hcp	hcp	-0.02	-0.02	-0.03	0.08

IV). In addition, the change in the oxygen threshold coverage where intermixing in the $\text{Cu}_x\text{Co}_{(1-x)}/\text{Cu}_{(1-x)}\text{Co}_x/\text{Co}(0001)$ system proceeds is increased only very slightly (4.4%) from 0.362 ML to 0.378 ML. The nonmixed $\text{Cu}_1 \text{ ML}/\text{Co}_1 \text{ ML}/\text{Co}(0001)$ surface would prefer to transition to the mixed $\text{Co}_{0.67}\text{Cu}_{0.33}/\text{Co}_{0.33}\text{Cu}_{0.67}/\text{Co}(0001)$ and the $\text{Co}_{0.33}\text{Cu}_{0.67}/\text{Co}_{0.67}\text{Cu}_{0.33}/\text{Co}(0001)$ alloys at oxygen coverages of 0.414 ML and 0.420 ML, respectively, for oxygen at the fcc surface sites.

In subsequent analyses, we probed the effect of the stacking pattern on the stability of the different Cu on Co surfaces reported above in both the absence and presence of oxygen. This effect was found to be insignificant. In the absence of oxygen, Co layers prefer hcp stacking, while the Cu layer prefers fcc stacking. The hcp stacking of $\text{Cu}_1 \text{ ML}/\text{Co}_1 \text{ ML}/\text{Co}(0001)$ denoted here as $\text{Cu}_1 \text{ ML}_{\text{hcp}}/\text{Co}_1 \text{ ML}_{\text{hcp}}/\text{Co}(0001)$ was therefore chosen as a reference state to evaluate the stability of other systems. The

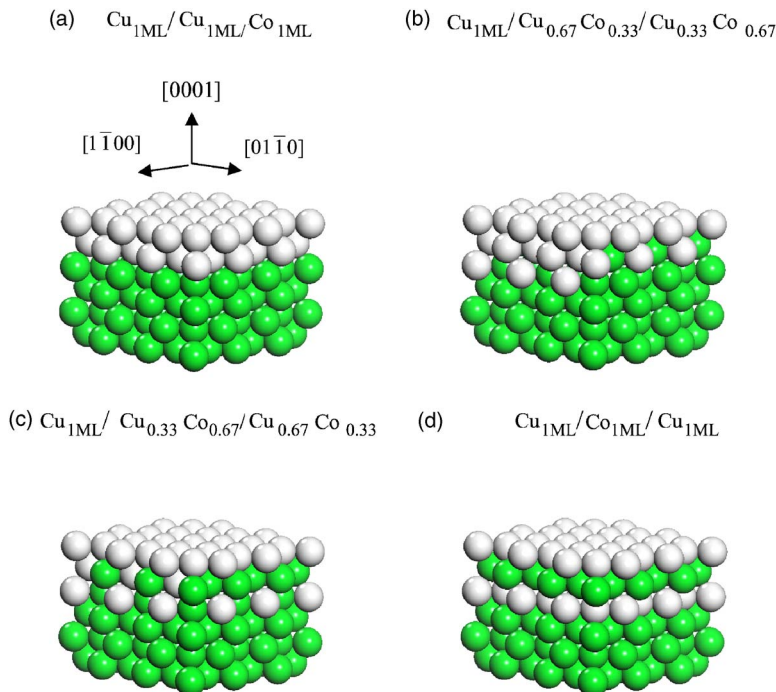


FIG. 6. (Color online) Side views of the Cu-capped various Cu/Co(0001) systems: (a) the Cu-capped nonmixed $\text{Cu}_1 \text{ ML}/\text{Cu}_1 \text{ ML}/\text{Co}_1 \text{ ML}/\text{Co}(0001)$ system, (b) the Cu-capped alloy-mixed $\text{Cu}_1 \text{ ML}/\text{Co}_{0.33}\text{Cu}_{0.67}/\text{Co}_{0.67}\text{Co}_{0.33}/\text{Co}(0001)$ system, (c) the Cu-capped alloy-mixed $\text{Cu}_1 \text{ ML}/\text{Co}_{0.67}\text{Cu}_{0.33}/\text{Co}_{0.33}\text{Cu}_{0.67}/\text{Co}(0001)$ system, and (d) the Cu-capped Co-capped $\text{Cu}_1 \text{ ML}/\text{Co}_1 \text{ ML}/\text{Cu}_1 \text{ ML}/\text{Co}(0001)$ systems. The light green spheres refer to the Co atoms whereas the white spheres refer to Cu atoms.

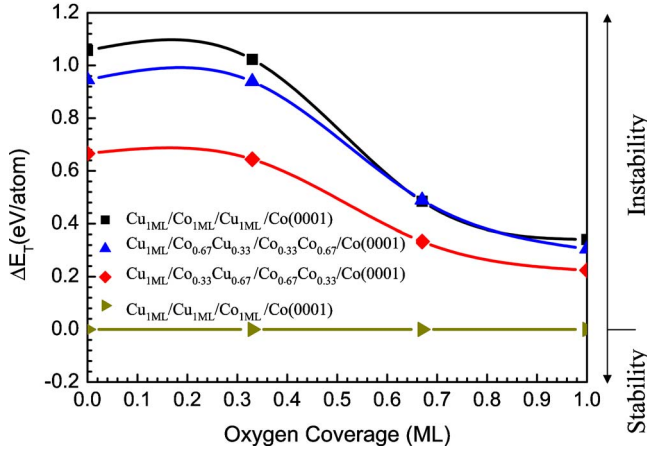


FIG. 7. (Color online) The influence of the oxygen coverage on the difference in the total energy ($\Delta E_{T,0}$) for Cu-capped various Cu/Co(0001) systems. The difference in the total energy between surfaces ($\Delta E_{T,0}$) is defined as the total energy ($E_{T,i}$) of the surface of interest minus that of the reference surface, that is, $\Delta E_{T,0} = E_{T,i} - E_{T,0}$. The reference surface used herein is the Cu-capped nonmixed $\text{Cu}_1 \text{ML}/\text{Cu}_1 \text{ML}/\text{Co}_1 \text{ML}/\text{Co}(0001)$ surface. The oxygen binds at the hcp threefold sites.

surface stability for a particular stacking pattern is defined as ΔE_T

$$\Delta E_T = E_{\text{Specific}}^T - E_{\text{Reference}}^T \quad (2)$$

which is the difference in the total energy for a specific stacking pattern minus the total energy of the reference system. For surfaces with ΔE_T values that are greater than zero, the hcp stacking is the most stable structure. The value of ΔE_T for the fcc stacking of the $\text{Cu}_1 \text{ML}/\text{Co}_1 \text{ML}/\text{Co}(0001)$ system denoted as $\text{Cu}_1 \text{ML}_{\text{fcc}}/\text{Co}_1 \text{ML}_{\text{fcc}}/\text{Co}(111)$ was found to be +0.04 eV/atom (Table V). The positive value here indicates that the hcp stacking is slightly more stable. On the other hand, if the Co layer takes on hcp stacking but the top Cu layer takes on fcc stacking [denoted as

$\text{Cu}_1 \text{ML}_{\text{fcc}}/\text{Co}_1 \text{ML}_{\text{hcp}}/\text{Co}(0001)$], then the value of ΔE_T is -0.01 eV/atom (Table V), which indicates that this mixed $\text{Cu}_{\text{fcc}}/\text{Co}_{\text{hcp}}/\text{Co}(0001)$ surface is slightly more stable. Similarly, the most stable structure for the capped $\text{Co}_1 \text{ML}/\text{Cu}_1 \text{ML}/\text{Co}(0001)$ system in the absence of oxygen is $\text{Co}_1 \text{ML}_{\text{hcp}}/\text{Cu}_1 \text{ML}_{\text{fcc}}/\text{Co}(0001)$, where the Co layer prefers hcp stacking while the Cu layer prefers fcc stacking.

The slight gain in energy induced by the Co-hcp and Cu-fcc stacking patterns is suppressed when oxygen was introduced to the surface. The metal-oxygen bonds are significantly stronger than the metal-metal bonds and can therefore act to overcome these small energy changes. For example, the energy difference reported in Table V between the $\text{O}_{\text{fcc}}/\text{Cu}_1 \text{ML}_{\text{hcp}}/\text{Co}_1 \text{ML}_{\text{hcp}}/\text{Co}(0001)$ and the $\text{O}_{\text{fcc}}/\text{Cu}_1 \text{ML}_{\text{fcc}}/\text{Co}_1 \text{ML}_{\text{hcp}}/\text{Co}(0001)$ surfaces are negligible. Similarly, the energy gain in comparing $\text{O}_{\text{fcc}}/\text{Co}_{\text{hcp}}/\text{Cu}_{\text{hcp}}/\text{Co}(0001)$ with $\text{O}_{\text{fcc}}/\text{Co}_{\text{hcp}}/\text{Cu}_{\text{fcc}}/\text{Co}(0001)$ is also very small (Table V). The main difference between the oxygen-covered Cu/Co(0001) systems were observed to be induced from the oxygen binding site.

Finally, we probed the influence of oxygen coverage on the growth of thicker Cu films on the Co substrate. In particular, we analyze various $\text{Cu}_1 \text{ML}/\text{Cu}_x \text{Co}_{(1-x)}/\text{Cu}_{(1-x)} \text{Co}_x/\text{Co}(0001)$ systems, where $x = 1.0, 0.67, 0.33, 0.0$, as shown in Fig. 6. The relative stability of these systems were established by calculating the total energy difference, ΔE_T , as shown in Fig. 7. The results in Fig. 7 show that the Cu-capped nonmixed $\text{Cu}_1 \text{ML}/\text{Cu}_1 \text{ML}/\text{Co}_1 \text{ML}/\text{Co}(0001)$ system is the most stable system over the full range of oxygen coverages (0.0 to 1.0 ML). The calculated binding energies for oxygen on the surface of these systems were very similar to that for the binding of oxygen on the $\text{Cu}_1 \text{ML}/\text{Co}_1 \text{ML}/\text{Co}(0001)$ system as indicated in Fig. 8. This suggests that the changes in the electronic structure and lattice structure are negligible over more than a few layers. The critical step in controlling intermixing during epitaxial growth of Cu on Co therefore appears to be at the initial monolayer coverage of Cu on Co. Thicker copper films are

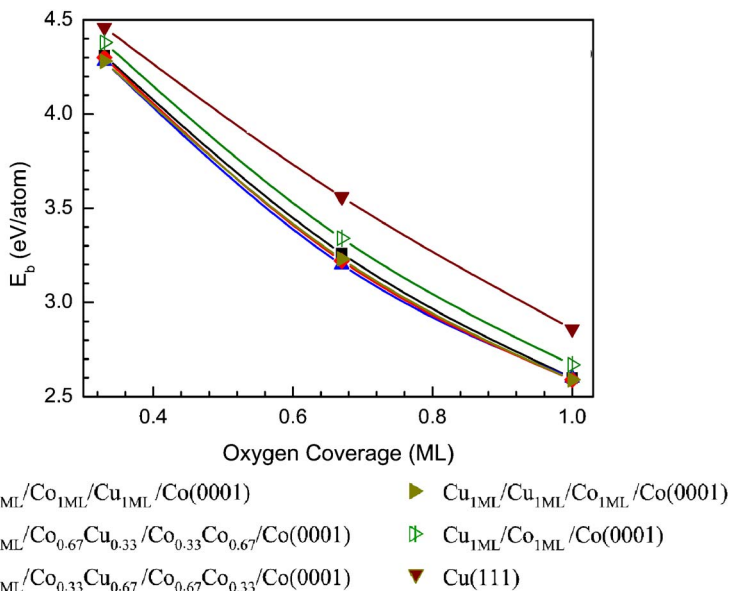


FIG. 8. (Color online) The correlation between the binding energy, E_b , in eV/atom of an adsorbed oxygen atom and the surface atomic oxygen coverage for the various $\text{Cu}_2 \text{ML}/\text{Co}(0001)$ surfaces. The oxygen coverage is varied between 0.33 ML to 1.00 ML.

TABLE VI. The effects of oxygen adsorption on the work function of the nonmixed $\text{Cu}_1\text{ML}/\text{Co}_1\text{ML}/\text{Co}(0001)$ and the Co-capped (mixed) $\text{Co}_1\text{ML}/\text{Cu}_1\text{ML}/\text{Co}(0001)$ systems. Atomic oxygen coverage varies from 0.0 ML to 1.0 ML.

Surfaces	Work function (eV)			
	Oxygen coverage (ML)			
	0.00	0.33	0.67	1.00
$\text{Co}_1\text{ML}/\text{Cu}_1\text{ML}/\text{Co}(0001)$	5.12	6.13	6.54	6.80
$\text{Cu}_1\text{ML}/\text{Co}_1\text{ML}/\text{Co}(0001)$	4.86	6.75	7.72	8.21

not as susceptible to oxygen-induced segregation of Co even at high oxygen coverages.

VI. EFFECTS OF OXYGEN ON THE SURFACE ELECTRONIC AND MAGNETIC PROPERTIES OF THE $\text{Cu}/\text{Co}(0001)$ SYSTEMS

A. Work function

The work function of the metal substrate is rather sensitive to the structural, electrical, chemical, and magnetic properties of surface layers and as such can be used as a probe of the influence of adsorbed oxygen. The nonmixed $\text{Cu}_1\text{ML}/\text{Co}_1\text{ML}/\text{Co}(0001)$ and the Co-capped (mixed) $\text{Co}_1\text{ML}/\text{Cu}_1\text{ML}/\text{Co}(000)$ shown in Figs. 2(a) and 2(d), respectively present the two extremes for the $\text{Cu}_1\text{ML}/\text{Co}(0001)$ systems analyzed herein and were therefore used as probe surfaces. The work function was calculated as the difference in the potential between the center of the vacuum of the slab and the Fermi energy. The results which are summarized in Table VI show that the work function for the Co-capped (mixed) $\text{Co}_1\text{ML}/\text{Cu}_1\text{ML}/\text{Co}(0001)$

surface increases from 5.12 to 6.80 eV as the oxygen coverage increases from 0.0 ML to 1.0 ML. The work function for the nonmixed $\text{Cu}_1\text{ML}/\text{Co}_1\text{ML}/\text{Co}(0001)$ surface, however, increased from 4.86 to 8.21 eV as the coverage was increased from 0.0 to 1.0 ML. The calculated values for the bare $\text{Co}_1\text{ML}/\text{Cu}_1\text{ML}/\text{Co}(0001)$ and $\text{Cu}_1\text{ML}/\text{Co}_1\text{ML}/\text{Co}(0001)$ surfaces were 5.12 and 4.86 eV, respectively. They are consistent with other DFT-calculated values reported in the literature for $\text{Co}(0001)$ (5.27 eV) and $\text{Cu}(111)$ (4.78 eV) surfaces.¹⁵ They are also consistent with experimental measures which range from 4.59 to 4.77 eV for Cu (Refs. 39–41) and 5.0 eV (Ref. 42) for Co. In both systems, the adsorption of oxygen leads to charge transfer from the metal to the oxygen which increases the work function of the metal.

B. Electronic structure

A detailed analysis of the electronic structure is provided for the nonmixed $\text{Cu}_1\text{ML}/\text{Co}_1\text{ML}/\text{Co}(0001)$ and the Co-capped (mixed) $\text{Co}_1\text{ML}/\text{Cu}_1\text{ML}/\text{Co}(0001)$ surfaces and for the influence of oxygen coverage on both of these surfaces. These two surfaces were, once again specifically examined since they provide the two extremes for Cu and Co surface segregation.

The changes in the electronic structure of the nonmixed Cu-segregated surface ($\text{Cu}_1\text{ML}/\text{Co}_1\text{ML}/\text{Co}(0001)$) are given in Figs. 9–11. The filling of the total density of states (DOS) was determined by calculating the fractional area under the DOS curves below the Fermi level. These results are presented in Tables VII and VIII.

The total density of states for the unmixed Cu-terminated [$\text{Cu}_1\text{ML}/\text{Co}_1\text{ML}/\text{Co}(0001)$] surface is presented in Fig. 9 and in Table VII as a function oxygen coverage. The results show that there is a small but general broadening of the bands with increasing oxygen coverage. A band at -17 eV below the Fermi level appears as the surface is exposed to

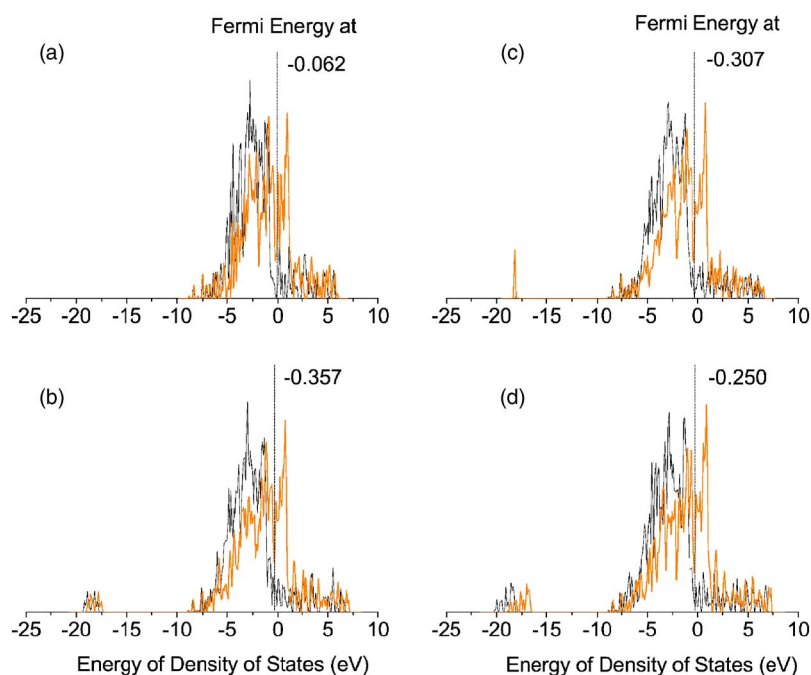


FIG. 9. (Color online) The density of states (DOS) for the $\text{Cu}_1\text{ML}/\text{Co}_1\text{ML}/\text{Co}(0001)$ system with various oxygen coverage: (a) 0 ML of atomic oxygen; (b) 0.33 ML of atomic oxygen; (c) 0.67 ML of atomic oxygen; and (d) 1.0 ML atomic oxygen. ML represents monolayer. Orange line represents DOS of spin-down electrons; black line represents DOS of spin-up electrons.

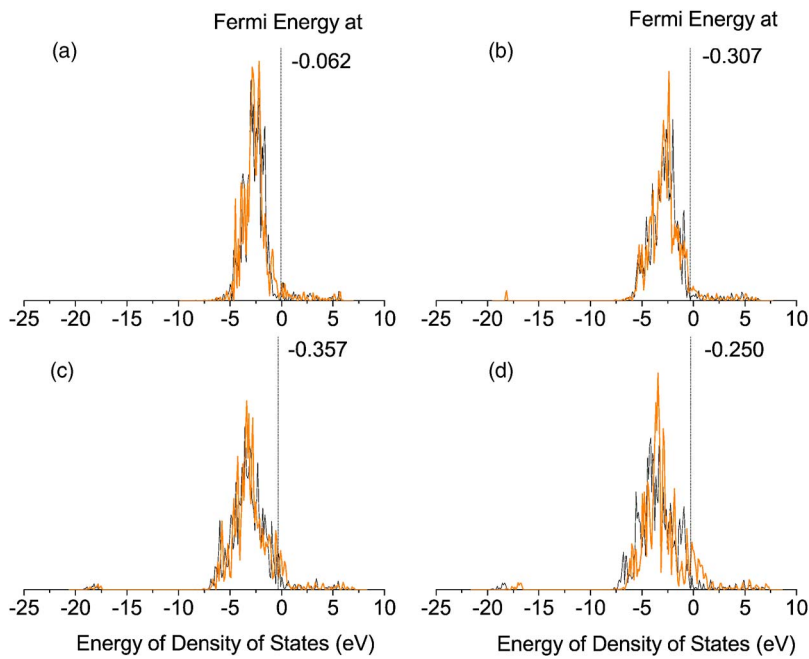


FIG. 10. (Color online) The partial density of states of the d band of the surface Cu atom for the $\text{Cu}_1 \text{ ML}/\text{Co}_1 \text{ ML}/\text{Co}(0001)$ system with various oxygen coverage: (a) 0 ML of atomic oxygen; (b) 0.33 ML of atomic oxygen; (c) 0.67 ML of atomic oxygen; and (d) 1.0 ML atomic oxygen. ML represents monolayer. Orange line represents DOS of spin-down electrons; black line represents DOS of spin-up electrons.

oxygen. The band is the result of the surface Cu-O bonds that form. It shifts to slightly lower energies and increases with increasing oxygen surface coverage. As the oxygen surface coverage increases, the minority band (shown in orange in Fig. 9) shifts away from the majority band (shown as the black line in Fig. 9) and also illustrated in the values reported in Table VII.

In general, it is difficult to distinguish the fine-scale individual changes in the overall band structure. We therefore analyzed the partial density of states in order to help separate out the changes in the electronic structure at the surface. The results in Fig. 10 show the partial density of states on the surface Cu atoms as a function of oxygen coverage. There is a general broadening in the distribution as the oxygen cov-

erage increases. The peak for both the majority and minority bands lie between -2.5 and -3 eV below the Fermi level. This is consistent with bulk fcc Cu which lies about -2 eV below the Fermi level for both the majority and minority electrons.⁴³ Both the majority and minority distributions shift to slightly lower energies with increasing O coverage as a result of bonding with oxygen. There is also some broadening in the partial density of states distribution due to the bonding of Cu with oxygen. The majority states on the surface Cu atoms remain constant while the minority states are slightly reduced as is shown in Table VIII. An analysis of the partial density of states (PDOS) of the subsurface Co atoms is shown in Fig. 11. The majority band for these Co atoms appears below the Fermi level whereas the minority band

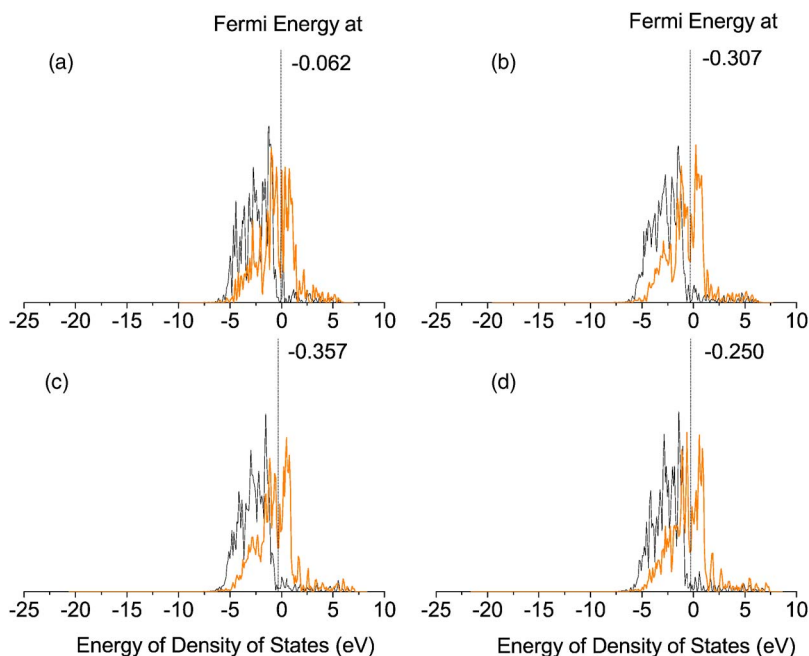


FIG. 11. (Color online) The partial density of states of the d band of subsurface Co atom for the $\text{Cu}_1 \text{ ML}/\text{Co}_1 \text{ ML}/\text{Co}(0001)$ system with various oxygen coverage: (a) 0 ML of atomic oxygen; (b) 0.33 ML of atomic oxygen; (c) 0.67 ML of atomic oxygen; and (d) 1.0 ML atomic oxygen. ML represents monolayer. Orange line represents DOS of spin-down electrons; black line represents DOS of spin-up electrons.

TABLE VII. The effects of the oxygen coverage on electronic properties of various Cu/Co(0001) systems: the filling factor of the DOS. The relative difference (Δd) for these properties is also calculated. This is defined as the difference between the values reported for minority spin electrons from those of the majority spin-up divided by the value of the property considered. A positive Δd value indicates that the property is greater for the majority over the minority spin.

Surfaces		Filling of DOS (fraction)			
		Oxygen coverage (ML)			
		0.00	0.33	0.67	1.00
Cu _{1 ML} /Co _{1 ML} /Co(0001)	Spin up	0.873	0.872	0.871	0.880
	Spin down	0.653	0.651	0.656	0.641
	$\Delta d(\%)$	25	25	25	27
Co _{1 ML} /Cu _{1 ML} /Co(0001)	Spin up	0.874	0.871	0.857	0.835
	Spin down	0.650	0.643	0.666	0.685
	$\Delta d(\%)$	26	26	22	18

appears above the Fermi level. This is consistent with bulk hcp Co which show the majority and minority bands at -1 eV and $+1$ eV, respectively.⁴³ The results for the d -band filling on the subsurface Co atoms indicate that there is little change in the filling of the majority states along with a small decrease in the minority states.

The detailed electronic structure for the Co-capped (Co_{1 ML}/Cu_{1 ML}/Co(0001)) mixed surface is presented in Figs. 12–14. The total density of states for the Co-terminated surface is shown as a function of oxygen coverage in Fig. 12. There is an evolution of peaks that grow in at -20 eV below the Fermi level that correspond to the formation of strong Co-O surface bonds. These states shift to lower energies with

increasing O coverage. The partial density of states plots on the surface Co and the subsurface Cu atoms provide a better breakdown for the contribution from the different metal layers. The density of states on the surface Co atoms (Fig. 13) shows a significant broadening in the d -band due to bonds that form between Co and atomic oxygen. The minority band shifts toward the majority band as these states become filled as a result of their interaction with oxygen. The splitting between the majority and minority bands is therefore significantly reduced as there is a significant decrease in the filling of the majority Co surface states as shown in Table VIII along with a significant increase in the filling of the minority Co states. The position of the d band for the majority and minority states begin to closely approach one another. The unpaired electrons on the oxygen atom begin to pair with the minority electrons of Co. This significantly reduces the magnetic moment and will likely reduce the spin scattering and the giant magnetoresistance of the surface layer. The PDOS on the subsurface Cu atoms is shown in Fig. 14 and the filling of these states is given in Table VIII. There does not appear to be much of a change in the subsurface PDOS of the Cu atoms.

C. Magnetic properties

Molecular oxygen is paramagnetic. Its adsorption and dissociation over Cu and Co lead to unpaired electrons that can significantly influence the magnetic properties of the surface. The overall magnetic moment of the system was calculated as a first measure of the influence of oxygen on these surfaces. The overall magnetic moment refers to the calculate magnetization of the entire unit cell of our calculated surface slab. In addition, we calculated the magnetic moment on individual atoms in different layers. The calculations of the magnetic moments were calculated by integrating the spin

TABLE VIII. The effects of the oxygen coverage on electronic properties of the surface and subsurface atoms for various Cu/Co(0001) surfaces: the filling factor of the DOS S . The relative difference (Δd) for these properties is also calculated.

			d -band filling (fraction)			
			Oxygen Coverage (ML)			
			0.00	0.33	0.67	1.00
Cu _{1 ML} /Co _{1 ML} /Co(0001)	Surface Cu atom	Spin up	0.959	0.950	0.928	0.950
		Spin down	0.949	0.935	0.889	0.860
		$\Delta d(\%)$	1	2	4	10
	Subsurface Co atom	Spin up	0.937	0.938	0.939	0.933
		Spin down	0.574	0.525	0.516	0.514
		$\Delta d(\%)$	39	44	45	45
Co _{1 ML} /Cu _{1 ML} /Co(0001)	Surface Co atom	Spinup	0.946	0.926	0.796	0.776
		Spin down	0.515	0.465	0.583	0.777
		$\Delta d(\%)$	46	50	27	0
	Subsurface Cu atom	Spin up	0.959	0.956	0.950	0.958
		Spin down	0.936	0.924	0.927	0.955
		$\Delta d(\%)$	2	3	2	0

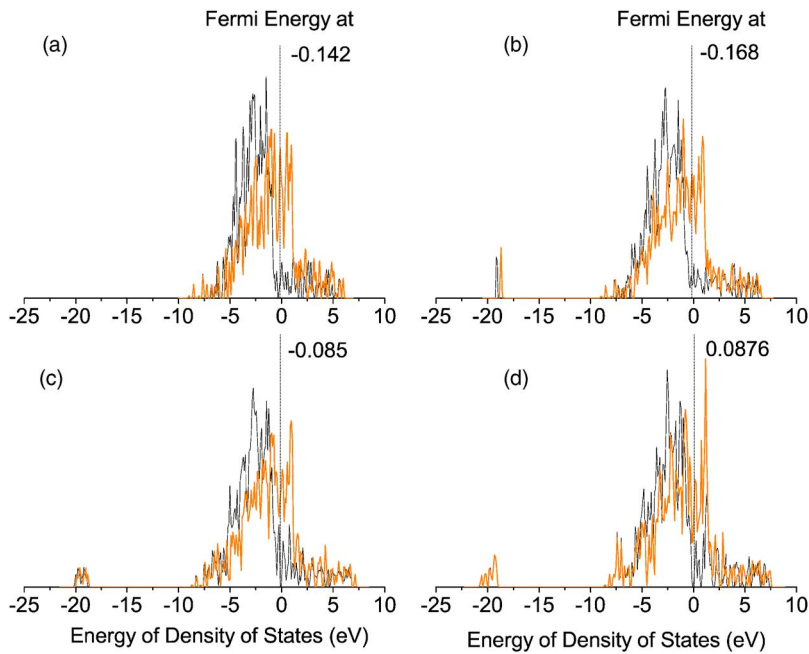


FIG. 12. (Color online) The density of states for the $\text{Co}_1 \text{ ML}/\text{Cu}_1 \text{ ML}/\text{Co}(0001)$ system with various oxygen coverage: (a) 0 ML of atomic oxygen; (b) 0.33 ML of atomic oxygen; (c) 0.67 ML of atomic oxygen; and (d) 1.0 ML atomic oxygen. ML represents monolayer. Orange line represents DOS of spin-down electrons; black line represents DOS of spin-up electrons.

density around each atom and subtracting the values for spin up (majority) density from spin down (minority) density. As a very simple approach we used atomic radii as cutoffs for the integration of spin density. The results provide good qualitative measures but should not be viewed as quantitatively accurate measures. We again focused solely the fully segregated Co-capped $[\text{Co}_1 \text{ ML}/\text{Cu}_1 \text{ ML}/\text{Co}(0001)]$ and the unmixed Cu-segregated $[\text{Cu}_1 \text{ ML}/\text{Co}_1 \text{ ML}/\text{Co}(0001)]$ surfaces. The discrete Fourier transform (DFT) calculated overall magnetic moment for the $\text{Co}_1 \text{ ML}/\text{Cu}_1 \text{ ML}/\text{Co}(0001)$ and $\text{Cu}_1 \text{ ML}/\text{Co}_1 \text{ ML}/\text{Co}(0001)$ systems are summarized in Table IX as a function of oxygen coverage. In addition, we report the results for an idealized Cu-segregated $\text{Cu}_1 \text{ ML}/\text{Co}_1 \text{ ML}/\text{Co}(0001)$ reference system. The magnetic properties

for this reference system were calculated by simply summing up the bulk magnetic properties on each atom, i.e., $1.6 \mu\text{B}/\text{atom}$ for Co, $0 \mu\text{B}/\text{atom}$ for Cu and $2 \mu\text{B}/\text{atom}$ for atomic oxygen.

The results indicate that the clean Co-capped $\text{Co}_1 \text{ ML}/\text{Cu}_1 \text{ ML}/\text{Co}(0001)$ and unmixed $\text{Cu}_1 \text{ ML}/\text{Co}_1 \text{ ML}/\text{Co}(0001)$ surfaces have similar overall magnetic moments at 19.94 and $19.75 \mu\text{B}/\text{system}$, respectively. These values are slightly greater than those reported for the ideal reference surface of $19.20 \mu\text{B}/\text{system}$. This suggests that the three-layer subsurface Co slab appears to have a higher magnetic moment than bulk Co.

As oxygen is added to the surface, the overall magnetic moments of the Co- and Cu-segregated surfaces, for fixed

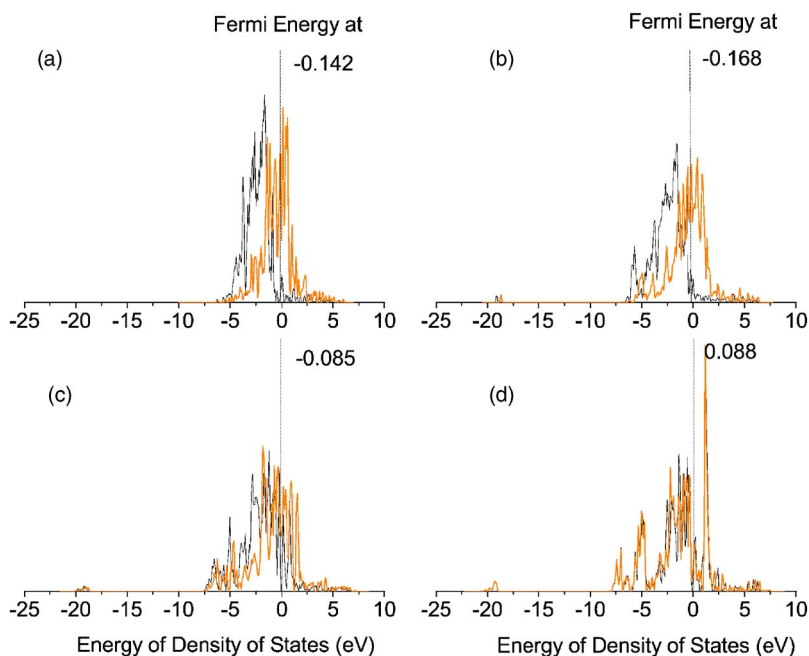


FIG. 13. (Color online) The partial density of states of the d band for the surface Co atom for the $\text{Co}_1 \text{ ML}/\text{Cu}_1 \text{ ML}/\text{Co}(0001)$ system with various oxygen coverage: (a) 0 ML of atomic oxygen; (b) 0.33 ML of atomic oxygen; (c) 0.67 ML of atomic oxygen; and (d) 1.0 ML atomic oxygen. ML represents monolayer. Orange line represents DOS of spin-down electrons; black line represents DOS of spin-up electrons.

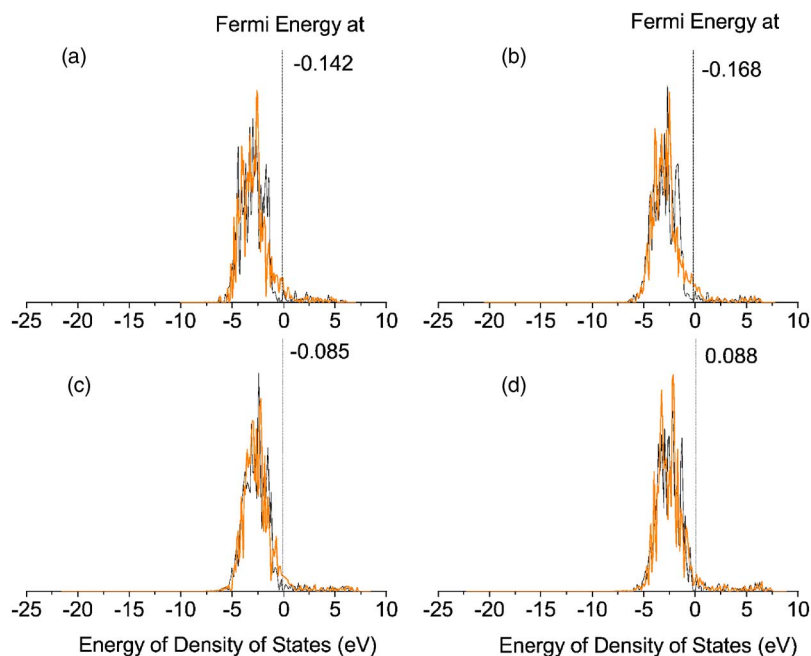


FIG. 14. (Color online) The partial density of states of the d-band for the subsurface Cu atom for the $\text{Co}_1\text{ ML}/\text{Cu}_1\text{ ML}/\text{Co}(0001)$ system with various oxygen coverage: (a) 0 ML of atomic oxygen; (b) 0.33 ML of atomic oxygen; (c) 0.67 ML of atomic oxygen; and (d) 1.0 ML atomic oxygen. ML represents monolayer. Orange line represents DOS of spin-down electrons; black line represents DOS of spin-up electrons.

oxygen coverages, are slightly lower than those for the reference systems which indicate that there is some quenching of the total surface and oxygen spin. At 0.33 ML oxygen coverage, for example we note that the ideal magnetic moment is $21.20 \mu\text{B}/\text{system}$ whereas that for the $\text{Co}_1\text{ ML}$ and the $\text{Cu}_1\text{ ML}$ surfaces were 20.50 and $20.54 \mu\text{B}/\text{system}$, respectively. This difference between the actual Co- and Cu-segregated surfaces and the ideal reference tends to increase with increasing oxygen surface coverage.

The addition of oxygen to the $\text{Co}_1\text{ ML}/\text{Cu}_1\text{ ML}/\text{Co}(0001)$ surface initially increases the magnetic moment of the surface when 0.33 ML oxygen were added. This indicates that the oxygen at lower surface coverage increases the magnetization. While the total spin of the atomic oxygen and slab surface is quenched (as indicated above), the initial addition of oxygen preserves some of its spin character. This is seen in the analysis of the magnetic moments on the oxygen and the surface Co atoms. At 33% the oxygen atoms retain a

TABLE IX. The DFT-calculated magnetic moment for $\text{Co}_1\text{ ML}/\text{Cu}_1\text{ ML}/\text{Co}(0001)$, $\text{Cu}_1\text{ ML}/\text{Co}_1\text{ ML}/\text{Co}(0001)$ surfaces and the reference $\text{Cu}_1\text{ ML}-\text{Co}_1\text{ ML}-\text{Co}(0001)$ system.

System		Magnetic moment			
		Oxygen coverage (ML)			
		0	0.33	0.67	1.000
$\text{Co}_1\text{ ML}/\text{Cu}_1\text{ ML}/\text{Co}(0001)$	Total system ($\mu\text{B}/\text{System}^a$)	19.94	20.50	18.42	16.00
	Adsorbed oxygen atom ($\mu\text{B}/\text{Atom}$)	-	0.18	0.06	-0.01
	Surface Co atom ($\mu\text{B}/\text{Atom}$)	1.75	1.76	0.94	-0.03
	Subsurface Cu atom ($\mu\text{B}/\text{Atom}$)	-0.02	0.01	0.02	0.00
	Bulk Co atom ($\mu\text{B}/\text{Atom}$)	1.65	1.64	1.73	1.68
$\text{Cu}_1\text{ ML}/\text{Co}_1\text{ ML}/\text{Co}(0001)$	Total system ($\mu\text{B}/\text{System}^a$)	19.75	20.54	21.35	24.10
	Adsorbed oxygen atom ($\mu\text{B}/\text{Atom}$)	-	0.01	0.17	0.69
	Surface Cu atom ($\mu\text{B}/\text{Atom}$)	-0.01	0.03	0.11	0.34
	Subsurface Co atom ($\mu\text{B}/\text{Atom}$)	1.62	1.73	1.75	1.73
	Bulk Co atom ($\mu\text{B}/\text{Atom}$)	1.70	1.71	1.72	1.71
$\text{Cu}_1\text{ ML}-\text{Co}_1\text{ ML}-\text{Co}(0001)^b$		19.20	21.20	23.20	25.20

^aNote: Both $\text{Co}_1\text{ ML}/\text{Cu}_1\text{ ML}/\text{Co}(0001)$ and $\text{Cu}_1\text{ ML}/\text{Co}_1\text{ ML}/\text{Co}(0001)$ systems contains 12 Co atoms and 3 Cu atoms per calculated unit cell. The oxygen coverage of 0.33, 0.67 and 1.0 ML corresponds to 1, 2, and 3 atoms per calculated unit cell, respectively.

^bThe $\text{Cu}_1\text{ ML}-\text{Co}_1\text{ ML}-\text{Co}(0001)$ system is a reference system. Its magnetic moment is calculated from the bulk magnetic moments of Co ($1.6 \text{ mB}/\text{atom}$) and Cu atom ($0 \text{ mB}/\text{atom}$) as well as the magnetic moment of oxygen atom ($2 \text{ mB}/\text{atom}$) in the vacuum.

portion of their magnetic character. In addition, the surface Co atoms retain their magnetic character. Therefore the initial addition of oxygen results in an increase in the magnetic moment. At higher coverages of oxygen, however, there is a significant decrease in the overall magnetic moment as the atomic oxygen atoms at the surface begin to spin pair with the magnetic Co atoms of the surface to quench their moments thus decreasing the overall magnetic moment of the surface. For example, at 1 ML coverage of oxygen, the magnetic moment of the Co-terminated surface decreases down to $16.00 \mu\text{B}/\text{system}$. The magnetic moments on the surface Co and adsorbed oxygen atoms are reduced to zero. These results are consistent with the speculated results presented in the section above on the changes in the overall electronic structure. The results are also consistent with recent experimental results by Morel *et al.*⁴⁴ who showed that oxygen at lower exposures initially induces an increase in magnetization on nanometer-sized cobalt particles. At higher oxygen exposures they find that there is a significant loss in magnetization which also nicely parallels the results found here.

The addition of oxygen to the $\text{Cu}_1 \text{ ML}/\text{Co}_1 \text{ ML}/\text{Co}(0001)$ surface acts to increase the overall magnetic moment of the surface. The magnetic moment for the 1 ML oxygen coverage for example is $24.1 \mu\text{B}/\text{system}$ which is significantly higher than the surface without oxygen ($19.75 \mu\text{B}/\text{system}$). The results for this surface tend to mirror the increases found for increasing oxygen on the bulk reference system. This indicates that the increase is likely due to an increase in the number of higher spin oxygen atoms at the surface which do not appear to lose their magnetic properties when they interact with the monolayer of Cu atoms at the surface. This is confirmed by the analysis of the magnetic moments on the surface oxygen as well as the other atoms. As oxygen coverage increases the magnetic moment from oxygen at the surface increases. There also appears to be an increase in the magnetic moment from the surface Cu atoms. The increase of spin on the Cu atom, however, could simply be due to the fact of the simple arbitrary delineation of the spin between the Cu-O bond used in calculating magnetic moments for the individual atoms.

VII. SUMMARY

The stability of the Cu/Co interface and its chemical composition largely depend on the processing conditions and the reaction environment that the surface is exposed to. As such, the surface composition can be manipulated by the addition of small amounts of oxygen. First-principle density functional theoretical calculations were used here to determine the influence of oxygen on the stability of the surface and establish the most favorable oxygen coverages to grow "ideal" thin films of Cu on Co(0001). The results indicate that in the absence of oxygen, the nonmixed $\text{Cu}_1 \text{ ML}/\text{Co}_1 \text{ ML}/\text{Co}(0001)$ interface is the most stable whereas the Co-terminated $\text{Co}_1 \text{ ML}/\text{Cu}_1 \text{ ML}/\text{Co}(0001)$ surface is the least stable. The mixed $\text{Co}_{0.33}\text{Cu}_{0.67}/\text{Co}(0001)$

and $\text{Co}_{0.33}\text{Cu}_{0.67}/\text{Co}_{0.67}\text{Cu}_{0.33}/\text{Co}(0001)$ alloys were found to be metastable. The stability of the surface increases with increasing the amount of Cu at the surface. This is largely due to smaller surface energy for Cu as compared to Co. In the absence of oxygen, Cu prefers to segregate out to the surface.

The binding energy for atomic oxygen on the ideal Co(0001) and Cu(111) yielded insight into the stability of each surface in the presence of oxygen. The magnitude for the binding energy of oxygen to the metal surface was found to predominantly depend on the nature of the metal atoms to which the oxygen binds. At the oxygen coverage of 0.33 ML, the binding energy for O on Co(0001) is 0.86 eV stronger than that for O on Cu(111). The difference in the binding energy of oxygen on Co versus Cu increases with increasing oxygen coverage. At 1 ML of oxygen, the difference in the binding energies of oxygen on Co(0001) and Cu(111) is about 1.67 eV. The oxygen binding energy, in general, increases with increasing the concentration of Co at the surface. The composition of the nearest neighbors either in the substrate or in the second atomic layer plays a secondary role.

For the different $\text{Cu}_x\text{Co}_{(1-x)}/\text{Cu}_{(1-x)}\text{Co}_x/\text{Co}(0001)$ systems studied herein, the presence of subsurface Cu increases the oxygen binding energy at the surface. The increase in the binding energy arises from changes in the electronic structure that shift the center of the *d* band of the metal slab projected onto the surface closer to the Fermi level.³⁷ Similarly, the binding energy for oxygen is weakened by an increase in the number of Co atoms in either the second layer below the surface or the substrate. Oxygen prefers to adsorb at the threefold fcc surface sites on all of the Cu/Co(0001) as well as the Cu(111) surfaces. Cu acts to influence the binding site preference at the surface. The differences in the binding energy between the fcc and hcp sites, $\Delta E_{b, fcc \rightarrow hcp}$, however, were found to be rather small ranging from 0.01 to 0.13 eV/atom.

The results described herein show that the addition of oxygen below 0.362 ML to Cu deposited on Co(0001) substrates will retain the unmixed surface Cu/Co(0001) surface. The magnetic properties of this surface improve with the addition of oxygen. Higher oxygen surface coverages lead to intermixing and the preferential segregation of Co to the surface. At these higher oxygen surface coverages the majority and minority bands begin to approach one another as there is substantial electron pairing. This leads to a significant decrease in the magnetization of the surface which would ultimately limit GMR performance.

ACKNOWLEDGMENTS

We wish to thank Qingfeng Ge, Xiaowang Zhou, Robert Johnson, Sanket Desai, Michael Palmer, and Chris Taylor for valuable technical discussions. This work was supported by DARPA through the Office of Naval Research (Contract No. N00014-98-C-0318).

*Author to whom correspondence should be addressed.

- ¹S. S. P. Parkin, R. Bhadra, and K. P. Roche, *Phys. Rev. Lett.* **66**, 2152 (1991).
- ²S. A. Wolf, D. D. Awschalom, R. A. Buhrman, J. M. Daughton, S. von Molnar, M. L. Roukes, A. Y. Chtchelkanova, and D. M. Treger, *Science* **294**, 1488 (2001).
- ³W. F. Egelhoff, P. J. Chen, C. J. Powell, R. D. McMichael, and M. D. Stiles, *Prog. Surf. Sci.* **67**, 355 (2001).
- ⁴D. J. Larson, A. K. Petford-Long, A. Cerezo, G. D. W. Smith, D. T. Foord, and T. C. Anthony, *Appl. Phys. Lett.* **73**, 1125 (1998).
- ⁵M. T. Kief and W. F. Egelhoff, *J. Appl. Phys.* **73**, 6195 (1993).
- ⁶J. Delafiguera, J. E. Prieto, C. Ocal, and R. Miranda, *Phys. Rev. B* **47**, 13043 (1993).
- ⁷M. T. Kief and W. F. Egelhoff, *Phys. Rev. B* **47**, 10785 (1993).
- ⁸A. Rabe, N. Memel, A. Steltenpohl, and T. Fauster, *Phys. Rev. Lett.* **73**, 2728 (1994).
- ⁹C. Tolkes, R. Struck, R. David, P. Zeppenfeld, and G. Comsa, *Phys. Rev. Lett.* **80**, 2877 (1998).
- ¹⁰Y. Wang, X. W. Li, J. F. Jia, H. Ji, Y. Yang, G. B. H., S. C. Wu, and R. G. Zhao, *Surf. Sci.* **375**, 226 (1997).
- ¹¹W. F. Egelhoff, P. J. Chen, C. J. Powell, M. D. Stiles, R. D. McMichael, J. H. Judy, K. Takano, and A. E. Berkowitz, *J. Appl. Phys.* **82**, 6142 (1997).
- ¹²W. L. Ling, Z. Q. Qiu, O. Takeuchi, D. F. Ogletree, and M. Salmeron, *Phys. Rev. B* **63**, 024408 (2001).
- ¹³W. L. Ling, O. Takeuchi, D. F. Ogletree, Z. Q. Qiu, and M. Salmeron, *Surf. Sci.* **450**, 227 (2000).
- ¹⁴X. W. Zhou, H. N. G. Wadley, R. A. Johnson, D. J. Larson, N. Tabet, A. Cerezo, A. K. Petford-Long, G. D. W. Smith, P. H. Clifton, R. L. Martens, and T. F. Kelly, *Acta Mater.* **49**, 4005 (2001).
- ¹⁵R. Pentcheva, and M. Scheffler, *Phys. Rev. B* **61**, 2211 (2000).
- ¹⁶S. Hope, M. Tselepi, E. Gu, T. M. Parker, and J. A. C. Bland, *J. Appl. Phys.* **85**, 6094 (1999).
- ¹⁷C. Tolkes, R. Struck, R. David, P. Zeppenfeld, and G. Comsa, *Appl. Phys. Lett.* **73**, 1059 (1998).
- ¹⁸T. Herrmann, K. Ludge, W. Richter, N. Esser, P. Pouloupoulos, J. Lindner, and K. Baberschke, *Phys. Rev. B* **64**, 184424 (2001).
- ¹⁹G. Boishin, L. D. Sun, M. Hohage, and P. Zeppenfeld, *Surf. Sci.* **512**, 185 (2002).
- ²⁰S. Miura, M. Tsunoda, and M. Takahashi, *J. Appl. Phys.* **89**, 6308 (2001).
- ²¹C. Tolkes, R. David, M. A. Krzyzowski, and P. Zeppenfeld, *Surf. Sci.* **454**, 741 (2000).
- ²²H. Wen, M. Neurock, and H. N. G. Wadley (unpublished).
- ²³W. Kohn and L. J. Sham, *Phys. Rev.* **140**, A1133 (1965).
- ²⁴P. Hohenberg and W. Kohn, *Phys. Rev.* **136**, B864 (1964).
- ²⁵G. Kresse and J. Hafner, *J. Phys.: Condens. Matter* **6**, 8245 (1994).
- ²⁶G. Kresse and J. Furthmuller, *Phys. Rev. B* **54**, 11169 (1996).
- ²⁷J. P. Perdew, J. A. Chevary, S. H. Vosko, K. A. Jackson, M. R. Pederson, D. J. Singh, and C. Fiolhais, *Phys. Rev. B* **46**, 6671 (1992).
- ²⁸D. Vanderbilt, *Phys. Rev. B* **41**, 7892 (1990).
- ²⁹H. M. Wen, M. Neurock, and H. N. G. Wadley (unpublished).
- ³⁰L. Z. Mezey and J. Giber, *Jpn. J. Appl. Phys., Part 1* **21**, 1569 (1982).
- ³¹R. Kern, G. Lelay, and J. J. Metois, edited by E. Kaldis (North-Holland, Amsterdam, 1979), Vol. 3, p. 1982.
- ³²G. L. Zhou, M. H. Yang, and C. P. Flynn, *Phys. Rev. Lett.* **77**, 4580 (1996).
- ³³M. O. Pedersen, I. A. Bonicke, E. Laegsgaard, I. Stensgaard, A. Ruban, J. K. Norskov, and F. Besenbacher, *Surf. Sci.* **387**, 86 (1997).
- ³⁴W. X. Li, C. Stampfl, and M. Scheffler, *Phys. Rev. B* **65**, 075407 (2002).
- ³⁵M. V. Ganduglia-Pirovano and M. Scheffler, *Phys. Rev. B* **59**, 15533 (1999).
- ³⁶C. Stampfl and M. Scheffler, *Phys. Rev. B* **54**, 2868 (1996).
- ³⁷B. Hammer and J. K. Norskov, in *Impact of Surface Science on Catalysis*, edited by H. Knozinger (Academic Press, San Diego, 2000), p. 71.
- ³⁸H. Wen, *Surfactant Effects on GMR Thin Film*, Ph.D. thesis, University of Virginia, Charlottesville, VA, USA, 2004, p. 230.
- ³⁹P. O. Gartland, S. Berge, and B. J. Slagsvold, *Phys. Rev. Lett.* **28**, 738 (1973).
- ⁴⁰G. A. Haas and R. E. Thomas, *J. Appl. Phys.* **48**, 86 (1977).
- ⁴¹G. G. Tibbets, J. M. Burkstrand, and J. C. Tracy, *Phys. Rev. B* **15**, 3652 (1977).
- ⁴²E. D. LIDE, in *Handbook of Chemistry and Physics* (CRC Press, 1992), p. 12.
- ⁴³R. Coehoorn, in *Magnetic Multilayers and Giant Magnetoresistance Fundamentals and Industrial Applications*, in Springer Series in Surface Sciences, edited by U. Hartmann (Springer, New York, 2000), Vol. 37, p. 73.
- ⁴⁴R. Morel, A. Brenac, and C. Portemont, *J. Appl. Phys.* **95**, 3757 (2004).
- ⁴⁵J. E. Prieto, C. Rath, S. Muller, R. Miranda, and K. Heinz, *Surf. Sci.* **401**, 248 (1998).